

Assessment of groundwater quantity, quality, and associated health risk of the Tano river basin, Ghana

Adwoba Kua-Manza Edjah¹ · Bruce Banoeng-Yakubo² · Anthony Ewusi³ · Enoch Sakyi-Yeboah⁴ · David Saka¹ · Clara Turetta⁵ · Giulio Cozzi⁵ · David Atta-Peters² · Larry Pax Chegbeleh²

Received: 7 August 2023 / Revised: 2 November 2023 / Accepted: 2 November 2023 / Published online: 28 November 2023
© The Author(s), under exclusive licence to Science Press and Institute of Geochemistry, CAS and Springer-Verlag GmbH Germany, part of Springer Nature 2023

Abstract In the Tano River Basin, groundwater serves as a crucial resource; however, its quantity and quality with regard to trace elements and microbiological loadings remain poorly understood due to the lack of groundwater logs and limited water research. This study presents a comprehensive analysis of the Tano River Basin, focusing on three key objectives. First, it investigated the aquifer hydraulic parameters and the results showed significant spatial variations in borehole depths, yields, transmissivity, hydraulic conductivity, and specific capacity. Deeper boreholes were concentrated in the northeastern and southeastern zones, while geological formations, particularly the Apollonian Formation, exhibit a strong influence on borehole yields. The study identified areas with high transmissivity and hydraulic conductivity in the southern and eastern regions, suggesting good groundwater availability and suitability for sustainable water supply. Secondly, the research investigated the groundwater quality and observed that the majority of borehole samples fall within WHO (Guidelines for Drinking-water Quality,

Environmental Health Criteria, Geneva, 2011, 2017. <http://www.who.int>) limit. However, some samples have pH levels below the standards, although the groundwater generally qualifies as freshwater. The study further explores hydrochemical facies and health risk assessment, highlighting the dominance of Ca–HCO₃ water type. Trace element analysis reveals minimal health risks from most elements, with chromium (Cr) as the primary contributor to chronic health risk. Overall, this study has provided a key insights into the Tano River Basin's hydrogeology and associated health risks. The outcome of this research has contributed to the broader understanding of hydrogeological dynamics and the importance of managing groundwater resources sustainably in complex geological environments.

Keywords Groundwater · Unsupervised machine learning technique · Hydrochemistry · Aquifer hydraulic parameter · Health risk

1 Introduction

Ghana, a tropical savannah country, faces challenges in meeting its water demands due to deteriorating quality of rivers and streams. Consequently, more than 80% of water supply comes from groundwater sources, primarily hand dug wells and boreholes (WRC 2012).

The Tano River Basin, one of the basins in Ghana, is no exception to this dependence on groundwater. However, rising demands for water, driven by population growth and industrial development like oil and gas and mining industries, have put tremendous pressure on the aquifers within the basin (Ghana Statistical Services, GSS, 2013, 2021). Sustainable Development Goal 6 emphasizes the need for

✉ Adwoba Kua-Manza Edjah
aedjah2@yahoo.co.uk

¹ Water Resources Research Centre, Ghana Atomic Energy Commission, Accra, Ghana

² Earth Science Department, University of Ghana, Legon, Accra, Ghana

³ Geological Engineering Department, University of Mines and Technology, Tarkwa, Ghana

⁴ Department of Statistics, University of Ghana, Accra, Legon, Ghana

⁵ Institute of Polar Sciences, National Research Council of Italy, Venice, Italy

providing portable water to all citizens by 2030. Achieving this goal in the Tano River Basin proves to be a challenging task, mainly due to insufficient hydrogeological information regarding both the quantity and quality of groundwater in the region. Important parameters like transmissivity, hydraulic conductivity, specific capacity, borehole depth, and yields are poorly known, hampering effective groundwater management. Another significant concern in the Tano River Basin is the degradation of groundwater quality. Research on the hydrochemistry of groundwater and its suitability for drinking is limited. The lack of data on chemical quality controlling groundwater chemistry further compounds the issue.

Insufficient understanding of groundwater contamination due to geogenic and anthropogenic activities hinders the usage of groundwater for various socio-economic purposes (Lutterodt et al. 2018; Affum et al. 2020; Cobbina et al. 2015; Nkansah et al. 2010; Edjah et al. 2021; Gyamfi et al. 2019; Doyi et al. 2018; Boateng et al. 2018). The potential adverse health effects of consuming groundwater contaminated with carcinogenic trace elements (e.g., chromium, arsenic), and nutrients (e.g., nitrate) are a cause for concern. Extended exposure to minimal levels of these contaminants can pose severe risks to human health (Radford et al. 2019). Several studies (e.g., Omeka and Egbueri 2022; Obasi and Akudinobi 2020; Nganje et al. 2019; Rahman et al. 2017; Adamu et al. 2015) have highlighted the toxicity of non-pathogens and pathogens when ingested through water or dermal contact. However, the specific impact on human health from drinking groundwater in the Tano River Basin remains unknown, despite studies conducted in other areas (e.g., Egbi et al. 2020; Anim-Gyampo et al. 2019; Doyi et al. 2018). The necessity of risk assessment and groundwater remediation before drinking is evident from the outcomes of these previous studies.

To address the knowledge gaps and potential risks, this study aims to comprehensively assess the quantity and quality of groundwater from boreholes in the Tano River Basin. The specific objectives include (1) estimation of the aquifer's hydraulic parameters using pumping test data, (2) using hydrochemical data to characterize the groundwater, and the controlling factors of the groundwater chemistry, and (3) using trace element data to investigate the associated human health risks from drinking the groundwater.

The findings of this study can establish a critical groundwater data bank for the Tano River Basin, providing valuable insights into the quantity, quality, and health risks associated with drinking ground water. Such knowledge is essential for the development of effective policies and measures to protect and sustainably manage the aquifers in the Tano River Basin in Ghana and beyond.

2 Research area and geological background

The rocks of the Tano River Basin are part of the Birimian Supergroup and the Apollonian Formation and are located between longitudes 2°05' and 2°35' west of the Greenwich meridian and latitudes 4°40' and 5°20' north of the equator. The Tano River Basin is located in the southwestern zone of Ghana and it is reachable from Takoradi, via the towns of Axim and Elubo border, as well as from Esiamia to Bomuakpole and Teleku-Bokazo to Salman all in the southwestern zone of Ghana.

The vegetation is classified as rainforest, and the main occupations of the inhabitants are fishing and coconut oil production. A limited number of young people work in the oil and mining industries, while the majority are involved in small-scale (illegal) gold mining activities. Tullow Oil, ENI, and Adamus Mining Resources, among other businesses, are amid those in the study's catchment area.

The research area's geological map is shown in Fig. 1. Geologically, the higher percentage of the study area is where the Birimian Supergroup rocks are found (Fig. 1). These rocks have several types of minerals (e.g., plagioclase, hornblende, micas, feldspars, ferromagnesian minerals, mafic minerals, sericite, and saussurite, among others). The rocks have considerable folds, foliations, joints, and weathering along fractures and other zones. The lower part of the map (Fig. 1) shows the rocks of the Apollonian Formation. These rocks overlay the Precambrian basement rocks of the western sedimentary basin of Ghana. The studies by Leube et al. (1990), Hirdes et al. (1992), and Taylor et al. (1992) provide more information on the geological time series of these rocks as well as how the rocks were formed. Generally, the transportation of groundwater within the Tano River Basin is primarily governed by the geological characteristics of the aquifer of the Apollonian formation and the Birimian supergroup rocks. The geological formation of these two aquifers often consists of sedimentary rocks, volcanic rocks, and fractured bedrock, which can have varying permeabilities and porosities (Leube et al. 1990, Hirdes et al. 1992, and Taylor et al. 1992). Hence, the flow of groundwater is influenced by hydraulic gradients, where water flows from areas of higher hydraulic head to areas of lower hydraulic head which will be explained further in subsequent chapters. The storage of groundwater in these two aquifers depends on their geological properties. Porous sedimentary layers like the rocks of the Apollonian can act as significant storage reservoirs for groundwater in the basin. Additionally, fractures and fissures in the bedrock of the Birimian supergroup can store water. The capacity for groundwater storage varies across different regions within the aquifer of the Apollonian Formation and the Birimian Supergroup

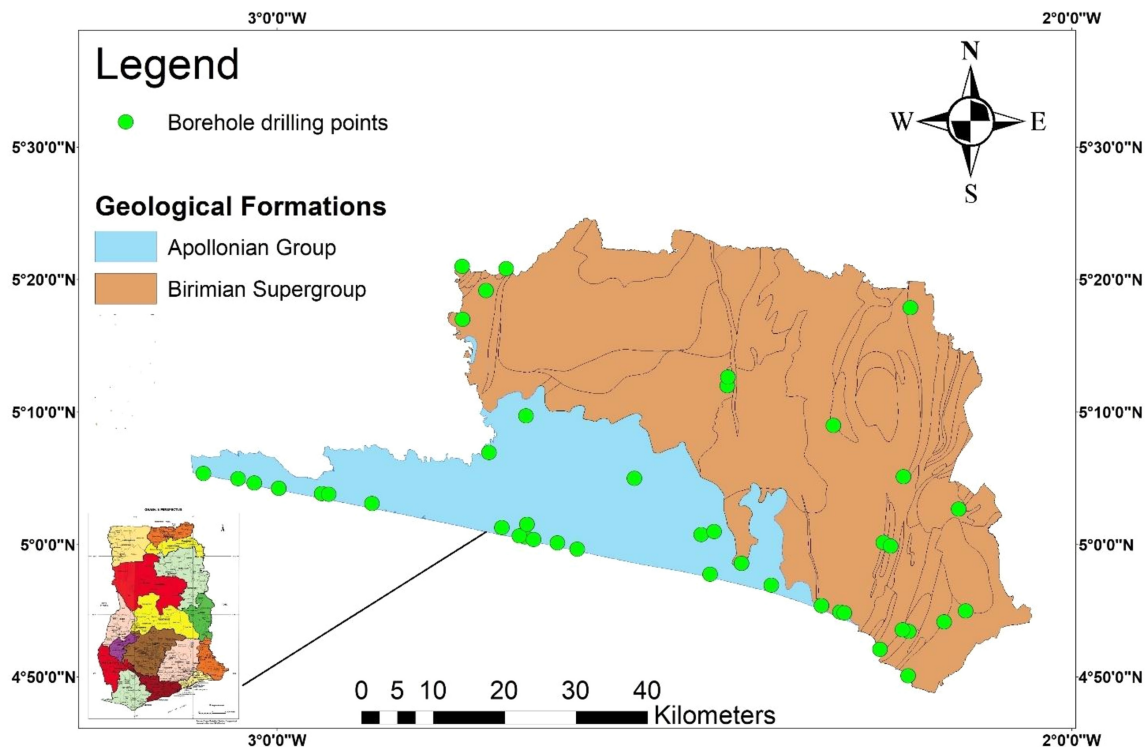


Fig. 1 Geological map of the study area with the borehole drilling points

due to variations in lithology and structural geology of the Tano River Basin. The distribution of groundwater to inhabitants of the study area is typically achieved through the development of boreholes, which tap into the aquifers of the Apollonian Formation and the Birimian Supergroup (WRC 2010). The depth and design of the boreholes are determined by the geological formations of the aquifer seen during drilling. The boreholes are fully mechanized and distribution networks are used to transport the borehole water to various communities, through Ghana water company pipelines (WRC 2010).

Since there are no existing studies on the flow, storage and distribution in the study area, this study being the first of its kind in the basin, will illustrate the flow of groundwater, and the outcome will contribute to the understanding of groundwater movement, and storage and this will aid in the development of groundwater management plans in the Tano River Basin.

3 Methods

3.1 Borehole drilling

Geophysical borehole siting was carried out at 55 sites across the study area (Fig. 1). 33 and 22 boreholes were successfully drilled and developed in the aquifers of the Apollonian Formation and the Birimian Supergroup of the

study area, respectively. During drilling, borehole logs were recorded and each borehole was cased and screened at water bearing zones.

3.2 Pumping test

In this study, pumping tests was conducted on the 55 developed boreholes to assess the characteristics of the aquifers (transmissivity, hydraulic conductivity and specific capacity) in the study area. The purpose of this test was to gain insights into the groundwater and make informed decisions for sustainable groundwater management with socio-economic implications. The methodology involved the following steps:

1. *Static water level measurement* Before starting the pumping tests, the initial static water level was measured in each borehole using a calibrated water level meter.
2. *Constant discharge test* For each borehole, a single well pumping test method was adopted. A pump with a specific horsepower per developmental yield was installed at a considerable depth within the borehole. The pump was powered by a generator to maintain a consistent discharge rate during the test.
3. *Data collection* During the pumping test, a 100-L calibrated bucket was used and a stopwatch was used to measure the discharge rate of water from the

borehole. Simultaneously, the drawdown (change in water level) at specified time intervals before and during pumping was recorded.

4. *Recovery phase* Following the discharge stage, the borehole was allowed to recover, and periodic water level measurements were taken at the same frequency as during pumping.
5. *Theis solution model* To analyze the data obtained from the pumping tests, Theis (1934) solution model was utilized. This model helped in the understanding of the aquifer's behavior and aided in the plotting of recovery and time drawdown curves for each borehole.
6. *Curve matching technique* To match the type curves (mathematical models) to the observed changes in water level, the curve matching technique was employed together with AQTESOLV 4.0 software.

The purpose of conducting a pumping test in this study is to gather quantitative data and insights into the hydrogeological properties and behavior of the aquifers of the Apollonian formation and Birimian supergroup rocks of the Tano River Basin. This information is vital for sustainable groundwater management, borehole design, environmental protection, and various other applications related to groundwater resources in the Tano River Basin.

3.3 Sampling

After the pumping test, all 55 boreholes were sampled following the sampling procedure described by Weaver et al. (2007) for the cations, anions, silica and trace elements. Physical parameters including temperature (T , °C), electrical conductivity (EC), total dissolved solids (TDS), pH, and salinity were determined in the field using a calibrated portable field meter. Alkalinity (as HCO_3^-) was measured in the field by the titrimetric method. The samples were collected in plastic polyethylene bottles, which were previously soaked in 10% nitric acid (HNO_3) for 24 h and rinsed severally with distilled water before sampling. At each borehole site, the bottles were washed with some of the borehole water before the bottles were filled. Five groups of borehole water were taken with a sterilized sampler at individually borehole location, together with duplicate borehole water. A 0.45 μm membrane filters were used to filter the borehole water into the sterilized polyethylene bottles. The borehole water sampled for the analysis of cation, silica and trace element was conserved by acidifying with 3 drops of 0.2 M HNO_3^- to achieve a pH of ≤ 2 . All the bottles containing the borehole water were labelled for cation, anion, and trace elements together with the dates and times of sampling and placed in a cooler with ice before being transported to the laboratories for analysis. The borehole water for the analysis of

microbiological loadings was sampled in sterilised glass bottles between 4:00 a.m. and 12:00 p.m. GMT in calm atmospheric environments with no rain showers (Engström et al. 2015). The bottles containing the water were kept in an ice chest with ice and then sent to the laboratory for microbiological analysis. At the laboratory, the borehole water samples were processed within five hours, and to prevent any external contamination, protective clothes were worn together with gloves. Also, the borehole water was collected through a sterilised tap attached to the borehole, and the water was allowed to flow for a maximum of 15 min before sampling for microbiological loading was done. The above-described methods aim to ensure the accurate and reliable analysis of various groundwater parameters, as well as to minimize the risk of contamination during the sampling and laboratory processes.

3.4 Analysis

Ion chromatography was used to analyze cations and anions, and an Inductively Coupled Plasma-Optical Emission Spectrometer (ICP-OES, PerkinElmer Co. Ltd., USA) was used to quantify the trace elements, and this was done at the laboratories of the Ghana Atomic Energy Commission and Ca' Foscari University of Venice, respectively. Double-distilled water was used for the preparation of the borehole water samples, and duplicates, standards, and blanks were run to ensure analytical accuracy. With data duplicability within 5%, the overall accuracy was less than 8% RSC (percent relative standard cations). To test the amount of silica in the water, a 410 nm wavelength solution, oxalic acid, and ammonium molybdate reagent were used. Without using additional chemicals to adjust for turbidity or colour, a blank was created. Before analysing the absorbance of samples of water that had been molybdate-treated, the analyser was set to zero absorbance. At the SGS laboratory in Tema, Ghana, silica concentration in borehole water was assessed using photometer calibration, and a control standard was developed for QC and QA purposes. Microbiological testing was done on the borehole water at the SGS Laboratory in Tema, Ghana and analysis was done based on APHA (1998). To stop microbial activity, samples were stored at 4 °C. Plate count, total coliforms, and *Escherichia coli* were all examined using the MPN approach. Analytical validation was carried out using internal reference material, and QA/QC was carried out using triplicate determinations. Duplicate analysis was used to calculate accuracy, and the %RSD was less than 8%. In order to evaluate the quality of the borehole water in the study region, water chemistry results, including trace elements, were used. Unsupervised machine learning algorithms were used to classify the

boreholes, and correlations between geology and anthropogenic sources were established. The processes controlling the groundwater quality were interpreted using Piper (1944) diagrams, bivariate plots, and principal component analysis (after Zumlot et al. 2013; Qin et al. 2013; Ranjan et al. 2013; Kolsi et al. 2013). The health risks of drinking groundwater were evaluated using trace element data. The effect of anthropogenic and natural activities on borehole water quality was evaluated using principal component analysis (PCA).

3.5 Data assessment procedure

3.5.1 Validation of data

To confirm the accuracy of the analytical findings, each water sample's ionic balance was assessed before analysis of the obtained data. The following is the ionic balance equation as stated by Freeze and Cherry (1979):

$$\text{Ionic Balance} = \frac{(\text{Sum of cations} - \text{Sum of anions})}{(\text{Sum of cations} + \text{Sum of anions})} \times 100$$

For analytical precision in cation and anion measurement, the IBE (ionic balance error) for the measured borehole water was computed based on the number of ions represented in milliequivalents per litre. The computed borehole water's IBE value was within a tolerance of 10% instead of 5%, which is likely a result of the absence of components such as nutrients, organic anions, and trace elements.

3.5.2 Data treatment

The data obtained from the laboratories were processed using different statistical methods like standard deviation, skewness, kurtosis, and mean. To determine whether the sample borehole water originated from a normal distribution, the skewness and kurtosis studies were performed. The hydrochemical, including trace element, concentrations of the borehole water were compared with WHO (2011) guidelines for drinking water quality. Using Kriging in ArcGIS 10.5, the spatial distribution of the estimated aquifer hydraulic parameters (transmissivity, hydraulic conductivity and specific capacity) was depicted. The underlying geology's porosity and permeability of the rocks led to the introduction of kriging. Additionally, Kriging was employed to create the spatial distribution maps because there was a very slim chance of drilling a dry well, or a borehole devoid of water in the study area. The creation of these maps will be a useful tool for managing water resources, planning land use, and making choices regarding aquifer utilisation. In addition, Microsoft Excel

2016 was used to perform the descriptive statistical analysis.

3.5.3 Mapping of borehole flow direction

The importance of predicting groundwater flow direction in advance was analysed using the Surfer 8 program and ModFlow software. Surfer 8 was used to interpret the XYZ data into clear surface map and ModFlow was used to develop the contour map. A contour map of the study area was generated using 55 XYZ data points of boreholes to determine the flow direction of the borehole water. The borehole contours (i.e., flow lines and equipotential lines) were digitized with Arc GIS 10.5 software. In general, the combination of Surfer 8 and ModFlow in predicting the groundwater flow direction and groundwater contour mapping enabled a comprehensive understanding of the subsurface hydrogeological conditions, which is vital for numerous applications in groundwater resources and management.

3.5.4 Water quality index (WQI)

Water quality index is an important method used to rate water quality. It covers the complex effect of several major water quality characteristics on the total water quality (Wu et al. 2005). The parameters employed reflect the impact of geogenic effects, natural variables, and anthropogenic activities on the quality of the borehole water. In calculating WQI for each drilled borehole, the measured physical parameters, cations, anions, and trace elements were considered. The weight for each parameter in the borehole water was allocated based on the relative importance of the measured parameters in the total borehole water quality for all socio-economic uses. Each measured parameter was given a weight that ranged from 1 to 5. The following equation was used to calculate relative weight:

$$W_i = wi / \sum_{i=1}^n wi \quad (1)$$

where W_i is the relative weight, wi is the weight of each parameter, n is the number of parameters.

The quality ranking scale for each parameter was calculated by dividing the content of each borehole water by its respective WHO (2011) standard. After, the result was multiplied by 100.

The above was represented by the equation

$$qi = \left(\frac{Ci}{Si} \right) * 100 \quad (2)$$

where qi = quality rating, Ci = the concentration of each parameter in each borehole water in mg/L. Si = the WHO

standard for each chemical parameter in mg/L according to the WHO (2011) guidelines.

The S_i is computed for each parameter in the final stage of WQI calculation. The WQI for each borehole is determined by adding the S_{li} values. Therefore, the following equation yields the S_{li} :

$$S_{li} = W_i * q_i \quad (3)$$

$$WQI = \sum S_{li} \quad (4)$$

where S_{li} is the sub-index of the i th parameter. Q_i is the rating based on the concentration of the i th parameter; n is the number of parameters.

In summary, the WQI will provide a single numerical value that will represent the overall water quality in each drilled borehole. Multiple water quality parameters, their relative importance, and how they compared to the WHO (2011) guidelines were taken into account. A higher WQI value indicates a better water quality, while a lower value suggests poorer water quality, which may require further investigation or mitigation measures.

3.5.5 Unsupervised machine learning technique

Under this section, the data structure (description or composition) and the procedure for clustering the borehole water based on the depth, yields, estimated aquifer hydraulic parameters, field parameters, cations, anions, trace elements, and microbiological loading were done using an unsupervised machine learning algorithm.

3.5.5.1 Data description and structure The data structure consists of a matrix-like structure where each row represents a borehole drilling point and each column represents the above-mentioned parameters used. After, a K-means algorithm is used for the classification of the parameters. The K-means cluster is a type of unsupervised learning process that learns from the data itself rather than from the labelled data. The K-means approach, which uses centroid-based clustering, establishes the distance between each of the aforementioned data sets and then assigns a centroid to the cluster. The rationale was to obtain the k -number of groups within each dataset. The procedure for using the K-means entails three stages, namely: (a) the pre-processing stage, (b) model building stage, (c) model evaluation stage. The pre-processing stage for this study involved the K-means algorithm being initialized using the Python programming language, based on the importations of relevant modules. The data set was imported and cleaned. In the model-building stage, the K-means algorithm needs the number of clusters, k , before the model can be built completely. Hence, for the determination of k , the specified range of values to estimate the inertia and silhouette scores

was assigned. The elbow plot (i.e., to find the optimal K for the dataset, where the elbow method is used, and the point where the decrease in inertia begins to slow) was constructed. Inertia and silhouette scores against the number of clusters were plotted. After determining the k clusters, the measured parameters were fitted to determine which cluster each of the 55 developed borehole points falls into. The labels (predictions) for each of the above-mentioned data sets were obtained from the pipeline. For the model evaluation stage, the principal component analysis (PCA) was used as the basis for evaluating the fitted model. The purpose was to ascertain whether the number of clusters used was appropriate given the dimensionality of the dataset.

3.5.6 Health risk assessment index

According to Li and Zhang (2010), Wu et al. (2009), De Miguel et al. (2007), and the USEPA (2004), a human health risk assessment is a technique used to assess the type and likelihood of harmful health consequences in persons who may be exposed to chemicals in polluted environments. The process is completed by employing the following four steps:

3.5.6.1 Identification of hazard No matter how hazardous some trace elements are, contaminants are thought to have an impact on human health. In this study, the measured trace elements are divided into two sections namely carcinogenic and non-carcinogenic.

3.5.6.2 Investigation of dose-response Under this section, the reference dose (RfD) was used to identify the precise relationship between the contaminant exposure dose and their influences. The United States Environmental Protection Agency's (USEPA 2004) publications served as the origin for the reference dosage (RfD) values used in this study.

3.5.6.3 Valuation of exposure The above was the process of estimating exposure factors quantitatively or qualitatively, including exposure pathways, body features, exposure occurrence, exposure period, etc. (USEPA 1986). In this study, dermal absorption and ingested exposure to groundwater were assessed. The standards for choosing the appropriate exposure frequency for people of the Tano River Basin have not yet been published because there have been no studies on dangers and environmental pollutants. As a result, data from US Environmental Protection Agency (USEPA 1986, 2004) were used as part of this study to determine exposure occurrence, body weight, ingestion rate, exposure period, and exposure time for individuals. Exposure dose for defining human health risk

through two pathways (ingestion and dermal) have been described in literature and could be calculated using Eqs. 5 and 6 as modified from the USEPA.

$$EXP_{ingestion} = \frac{C_{water} \times IR \times EF \times ED}{BW \times AT} \quad (5)$$

$$EXP_{dermal} = \frac{C_{water} \times SA \times Kp \times ET \times EF \times ED \times CF}{BW \times AT} \quad (6)$$

where, EXP is the exposure dose contacted through ingestion of borehole water ($EXP_{ingestion}$) and dermal absorption (EXP_{dermal}) and both are in units of mg/Kg/day. C_{water} is the average concentration of trace elements in the borehole water measured in mg/L. IR is the drinking water ingestion rate, which is considered 5 L/day (3.5 L/day for adult, 1.5 L/day for children) for this research. EF is the exposure frequency, which is assumed to be 365 days/year for this work. ED is the exposure duration, which is 76 years (70 years for adults and 6 years for children) for this study.

BW is the average body weight, that is, 85 kg (15 kg for children and 70 kg for adults). AT is the averaging of 27,740 days (2190 days for children and 25,550 days for adults) for both carcinogenic and non-carcinogenic. SA is the exposed skin area, which is 24,600 cm² (6600 cm² for children and 18,000 cm² for adults). Kp is the dermal permeability constant measured in cm/h and the Kp for the elements are 0.002 for Cr, 0.0027 for As, 0.002 for Ni, 0.0004 for Co, 0.0006 for Zn: 0.001 for Ba, Cu, B, Mn, Fe, Ni, Pb, Cd, Se, Ag, Sr, Ti, V, and Al, ET is the exposure time of 0.2 h/day, selected for this study. CF is the unit conversion factor, with the borewater chosen as 1L = 1000 cm⁻³.

3.5.6.4 Description of risk By integrating the data gathered from earlier steps, a quantitative description of the risk's magnitude and uncertainty was undertaken. By contrasting the predicted contaminant exposures from each exposure pathway (ingestion and dermal) with the reference dose (RfD) using Eq. 7, potential non-carcinogenic concerns resulting from exposure to parameters were identified.

$$HQ_{ing/derm} = \frac{EXP_{ing/derm}}{RfD_{ing/derm}} \quad (7)$$

RfD is the reference dose for diverse analyses (ingestion/dermal toxicity reference dose), which is based on US risk-based assessment and it is computed in mg/kg/day. Values for HQ is shown in Table 1.

11 trace element values out of the 18 analysed elements were computed for the reference dose (RfD) and the calculations were done based on US risk-based assessment, and the units are in mg/kg/day (Table 2).

Table 1 Hazard quotient (HQ)

HQ	Risk
< 1b	The risk is acceptable
≥ 1b	The risk is not acceptable

^bEPA is the Drinking water standards and health risk (USEPA 2004)

4 Results and discussion

4.1 Estimation of aquifer hydraulic parameters

In this section, the results of the computed aquifer hydraulic parameters are discussed, and Table 3 gives the statistical summary. According to Table 3, the minimum and maximum borehole depths are 18 and 62 m, respectively. From the spatial distribution map (Fig. 2) it is observed that the boreholes drilled in the northeast and south-eastern zones of the research region, with a few in the southwestern and northwest zones, have the deepest depths ($D = 49\text{--}62$ m). The rock formation of these boreholes belong to the rocks of the Birimian Supergroup with a few in the rocks of the Apollonian Formation (Fig. 1) of the study area and these rocks are consolidated or well fractured. The yields of the drilled boreholes range from 10 to 800 L/min (Table 3), and the boreholes with the highest yields ($Y = 463\text{--}800$ L/min) are situated in the coastal zone of the study area and are underlain by the rocks of the Apollonian Formation (Fig. 3). These rocks contain limestones, marl, mudstones with intercalated sandy beds (Fig. 1) and are highly porous and permeable. Figure 3 also suggests that a correlation exist between the drilling locations of the high yielding boreholes and the underlying geology. Additionally, a plot of the yields versus the borehole depths (Fig. 4) demonstrates a likely potential for decreased yields when the boreholes are drilled deeper, and this is likely related to the regional geological formations or conditions of the Tano River Basin.

For the aquifer hydraulic parameters, specifically transmissivity, hydraulic conductivity and specific capacity, the transmissivity values range from 1.73 to 1219.70 m²/day (Table 3). This suggests that the Tano River Basin have a high potential for groundwater flow and abundant borehole water. The highest transmissivity zone ($T = 545\text{--}1219.70$ m²/day) is found in the southern, and south-eastern areas, with other high varying values ($T = 113\text{--}545$ m²/day) across the study location (Fig. 5). The variability in transmissivity values across the study location indicates that different areas within the basin may have varying levels of groundwater productivity. Overall, the aquifers in the Tano River Basin seem to be highly productive, making them valuable for water supply purposes.

Table 2 The RfD of non-carcinogenic and carcinogenic parameters

Non-carcinogenic	Ba	Pb	Se	Zn	Carcinogenic	Cd	Cr	Co	Cu	Mn	Fe	Ni
RfD _{ingestion} (mg/Kg/day)	70	1.4	5	300		0.5	3	0.3	40	5	300	20
RfD _{dermal} (mg/Kg/day)	14	0.4	2.2	60		0	0	0	12	0.8	45	5.4

Table 3 Descriptive statistics of the estimated aquifer hydraulic parameters

Parameters	Specific capacity (L/min/m)	Aquifer thickness (m)	Hydraulic conductivity (m/day)	Static water level (a.m.s.l)	Transmissivity (m ² /day)	Depth (m)	Yields (L/min)
Number of samples	55	55	55	55	55	55	55
Mean	18.80	45.45	5.70	5.17	205.96	37.67	205.33
Minimum	0.72	19.00	0.04	− 0.80	1.73	18.00	10.00
Maximum	122.24	59.00	44.35	20.70	1219.70	62.00	800.00
Sum	545.28	1318.00	165.39	599.72	5972.91	1959.00	10,677.00
Confidence level (95.0%)	11.57	4.36	3.39	0.78	102.48	4.29	51.70

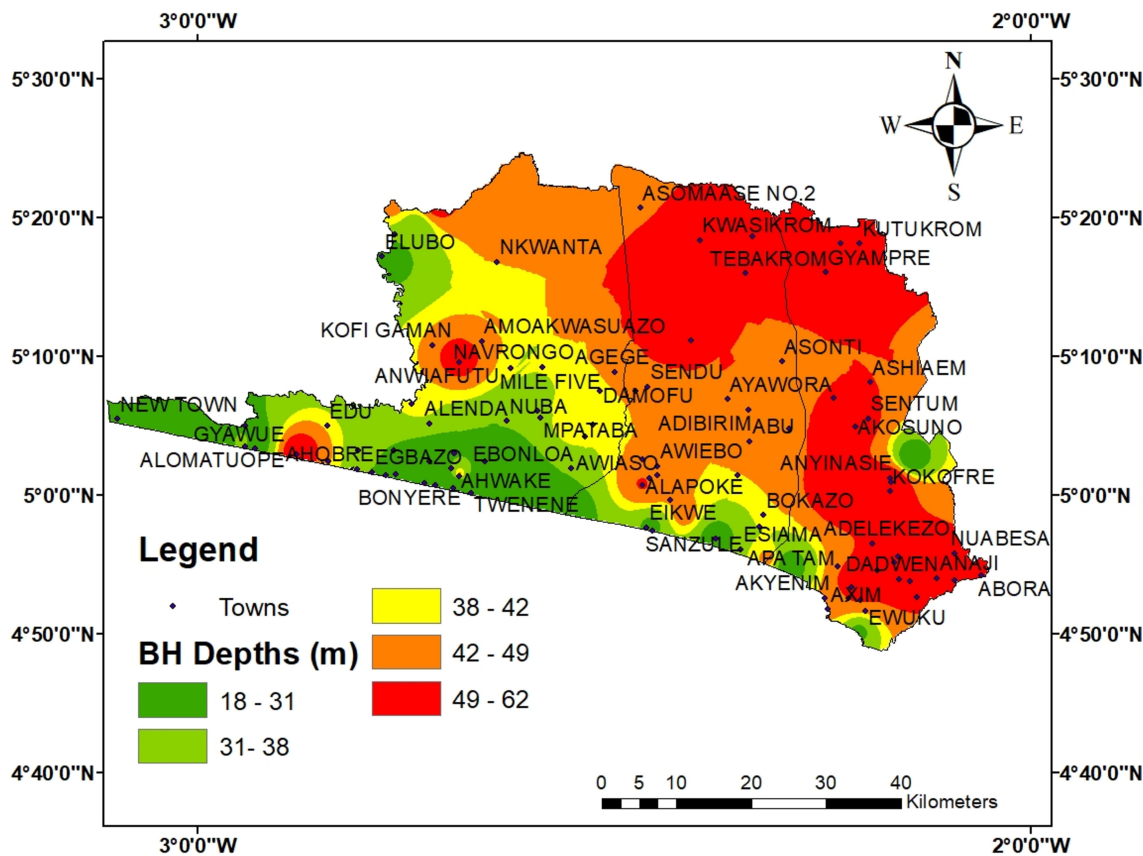


Fig. 2 Spatial distribution map showing the depth of the borehole

The hydraulic conductivity values for the drilled boreholes range from 0.04 to 44.35 m/day (Table 3) indicating spatial heterogeneity in the subsurface properties. In average, the subsurface materials in the study area allow

water to flow at a rate of approximately 5.70 m/day (Table 3). The lowest hydraulic conductivity (0.04–6.02 m/day) are observed in various locations across the study area (Fig. 6). The observed hydraulic

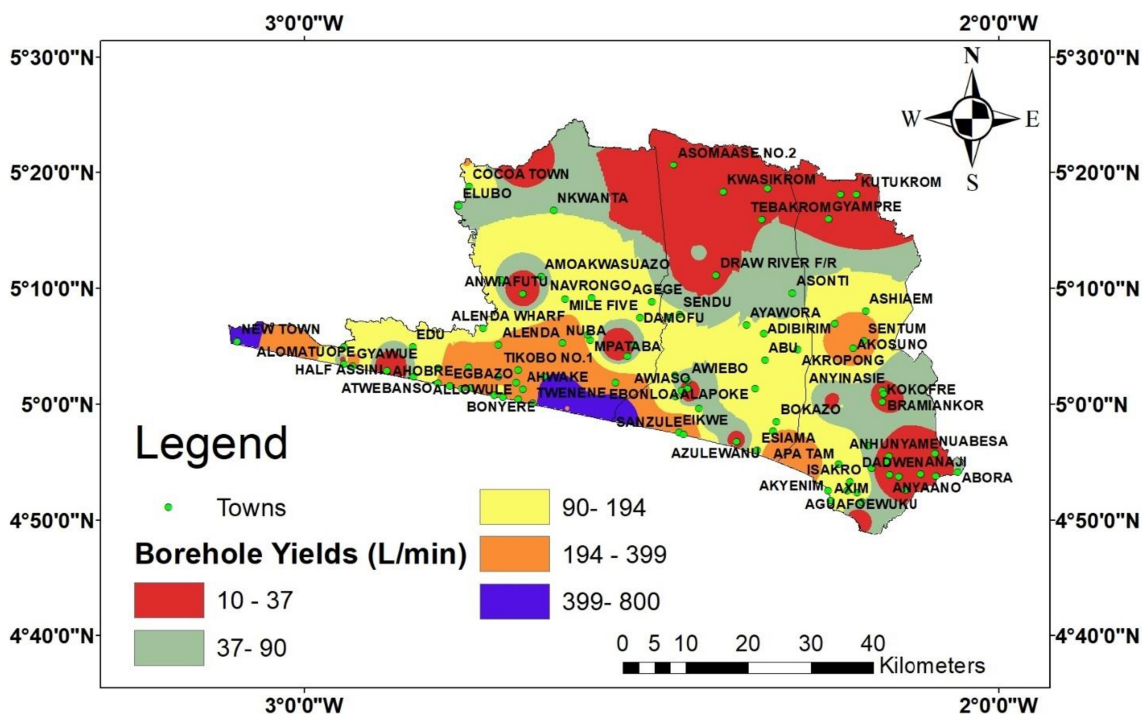


Fig. 3 The research area’s spatial distribution of borehole yields

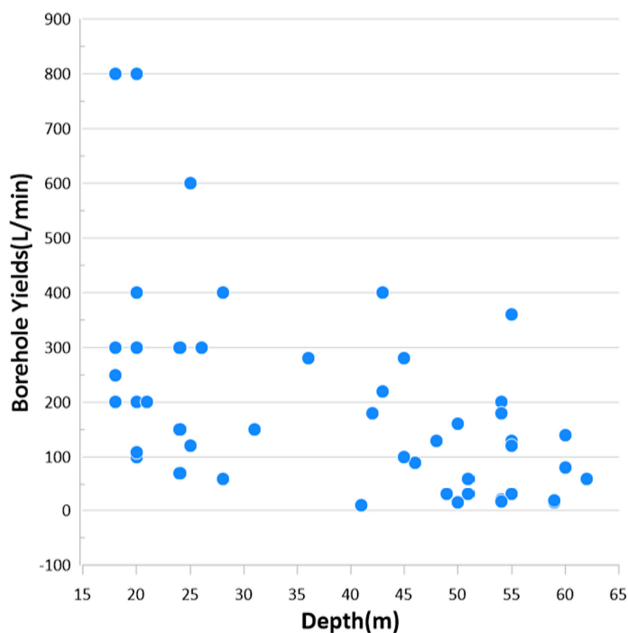


Fig. 4 Plot of borehole yields against the depths

conductivity values in this range suggest the southern, middle, south-eastern, northern, northeastern, western, southern, southwestern and north western areas of the Tano River basin have relatively impermeable subsurface materials. These areas are less capable of transmitting groundwater efficiently and are likely locations where groundwater discharge occurs. In other words, they

represent zones where groundwater is more likely to be extracted. Additionally, the highest hydraulic conductivity (14.79–44.35 m/day) zones are present in the southern, and south-eastern (Fig. 6), suggesting highly permeable subsurface materials. In addition, groundwater flows more easily through these zones, and they are considered suitable for groundwater recharge. This means that when rainwater or other sources of water infiltrate the ground, these zones allow for efficient replenishment of the aquifers.

The specific capacity values of the boreholes in the study area range from 0.72 to 122.24 L/min/m, with an average of 18.80 L/min/m (Table 3). According to the classification by Johnson et al. (1966), the boreholes are categorized into three groups: those yielding enough water for domestic use only ($SC < 12$ L/min/m). These boreholes which are less productive are seen across the study location (Fig. 7) and are less productive meaning they yield less water per unit drawdown. The second group are boreholes which offer a slightly higher water yield (12 L/min/m $\leq SC \leq 17$ L/min/m) compared to the previous group but are still limited in capacity. These boreholes are observed in the north western, north eastern, eastern, south eastern, middle and south western zone of the study area (Fig. 7). In addition, these boreholes can be used for small-scale irrigation or other modest water requirements. The final group are boreholes which are capable of providing water ($SC \geq 17$ L/min/m) for all socio-economic uses. These boreholes are seen in the southern, south east and

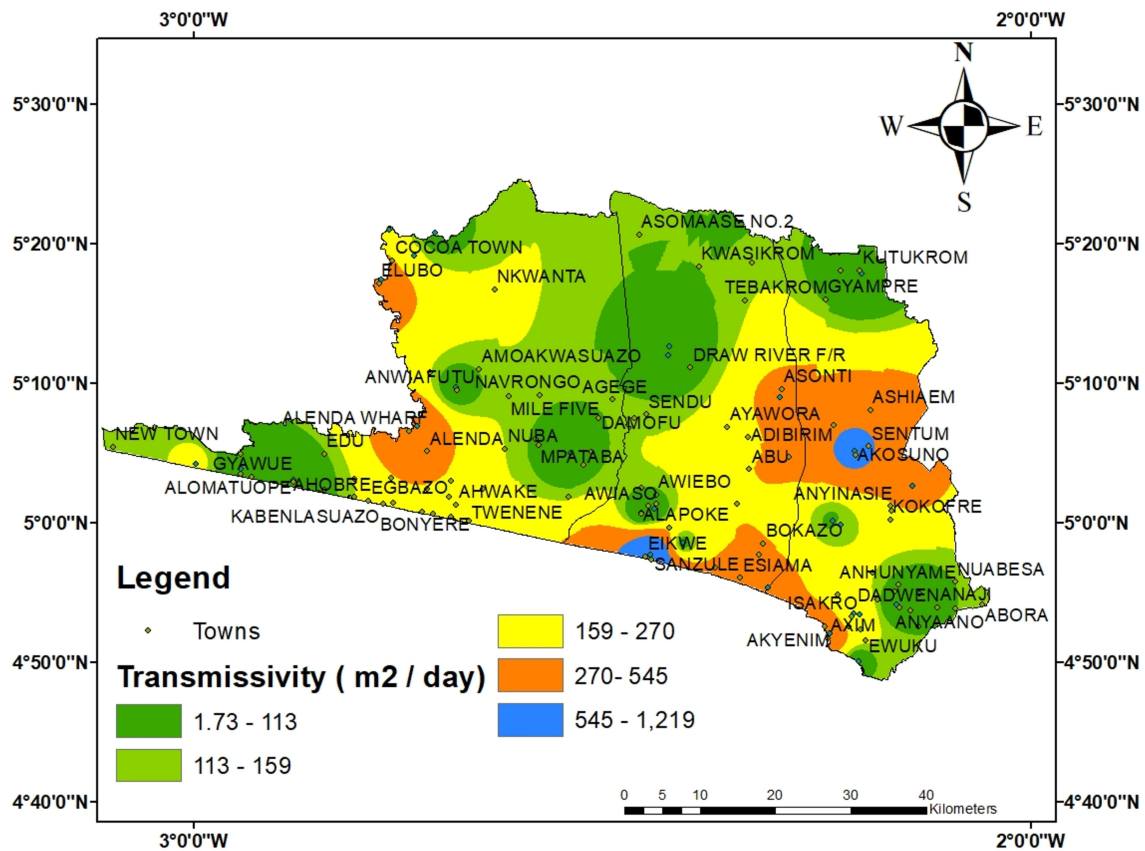


Fig. 5 Spatial distribution map of transmissivity for the study area

western zones of the study area (Fig. 7). Also, these boreholes are considered to have excellent groundwater productivity and are suitable for a sustainable groundwater extraction. They can also meet the demands of a variety of socio-economic activities, including agriculture, industrial processes, and domestic.

The direction of groundwater flow can be understood in the fact that groundwater always moves in the direction of decreasing hydraulic head. In this study, the measured static water levels ranged from -0.8 b.m.s.l to 20.70 a.m.s.l., with an average of 5.17 a.m.s.l. A hydraulic head map (also known as a water contour map) was produced using the static water levels (hydraulic heads) (Figs. 8, 9). The maps (Figs. 8, 9) show a regional groundwater flow from the recharge area around the north-west, southern and western (These areas have higher hydraulic head values compared to their locations) and flows towards the discharge areas around the south-east, and western. These areas have lower hydraulic head values compared to the recharge areas. In general, the groundwater flow direction in the Tano River Basin is from the higher hydraulic head recharge areas as stated above to the lower hydraulic head discharge areas. This flow pattern replicates the groundwater flow within the aquifers of the Apollonian formation

and the Birimian supergroup. This is a fundamental aspect of the Tano River basin hydrogeology which is unknown. Hence, this will aid in the effective and sustainable management of groundwater resources in the basin.

With a perfect correlation coefficient of 0.98 , a graph of the computed hydraulic heads against the surface elevation provides an illustrative knowledge of the aquifer's behaviour (Fig. 10) in the study location. In addition, the slope (0.8) (Fig. 10) and the direction of flow revealed that the groundwater in the Tano River Basin is flowing from a topographically higher elevation to a lower elevation. As such, the groundwater in the lower elevation that is areas underlain by the rocks of the Apollonian formation might be at risk of leachates and pathogens due to the unconsolidated rocks of the Apollonian and the deposition environment. Overall, a specific groundwater flow pattern being the first to be determined in the study location has been identified, and the obtained results is valuable for the understanding of aquifer behaviour of the Tano River Basin as well as identifying potential risks to the groundwater quality which will be discussed in subsequent chapters.

In conclusion, the assessment of aquifer hydraulic parameters within the Tano River Basin provides vital

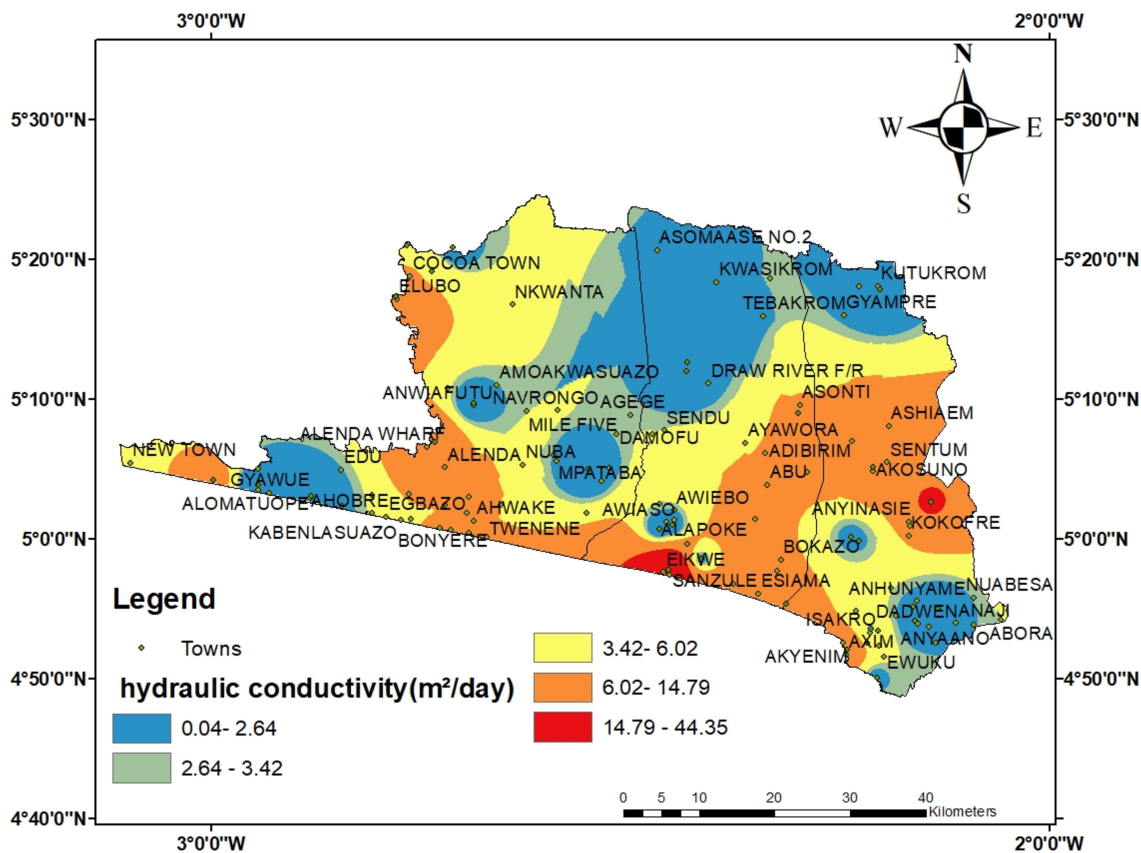


Fig. 6 Spatial distribution map of hydraulic conductivity for the study area

insights into the dynamic nature of the region’s hydrogeology. The observed changes in these hydraulic parameters signify a notable transformation in the groundwater, reflecting changes in local groundwater productivity, extraction patterns, and flow dynamics. Notably, the indication of good permeability and favourable hydraulic characteristics in especially areas underlain by the rocks of the Apollonian formation suggests potential opportunities for sustainable water supply. Conversely, areas underlain by the rocks of the Birimian Supergroup displaying lower hydraulic values necessitate careful planning to optimize groundwater utilization.

4.2 Hydrochemical characteristics of groundwater and its suitability for drinking

Under this specific objective, the characteristics of borehole water in the Tano River Basin is discussed. From the result of the analysed field parameters for the borehole water samples, it was seen that the pH data showed a mean of 6.69 and a median of 6.91 (Table 4), and the overall data indicates acidic to slightly basic water. A small percentage (4.8%) of boreholes had pH values below the WHO (2011) drinking water limit of 6.5–8.5. The borehole water’s acidity is

attributed to the oxidation and hydrolysis of pyrite (Preda and Cox 2000) in the study area. Luebe et al. (1990) and Atta-Peters and Garrey (2014) discovered nodules of pyrite in the underlying geology of the study area. Another contributor is rainwater infiltration. In the Tano River Basin, Edjah et al. (2015, 2019) observed that the source of groundwater recharge was of meteoric origin. CO₂ gas from cellular respiration (Isa et al. 2012) in the forested canopy of the study area is also another contributing factor. Additionally, clay minerals acting as H⁺ buffers (Sjöström 1993) are also another contributing factor to the low pH recorded in the groundwater. In the underlying geology of the study area, clay minerals such as kaolin, silica, etc. exist. The total dissolved solutes (TDS) in the groundwater had an average concentration of 114.11 mg/L, and the overall data (Table 4) indicates fresh groundwater. According to WHO (2011), groundwater is typically categorised into three groups: fresh water (TDS < 1000 mg/L), salt water (3000 < TDS < 10000 mg/L), and brackish water (1000 < TDS < 3000 mg/L). From the above divided, the TDS data for the boreholes are all below 1000 mg/L. This might be attributed to minimal contamination from anthropogenic sources or geologic weathering, and short residence time. In general, lower TDS values are linked with decreased mineral content

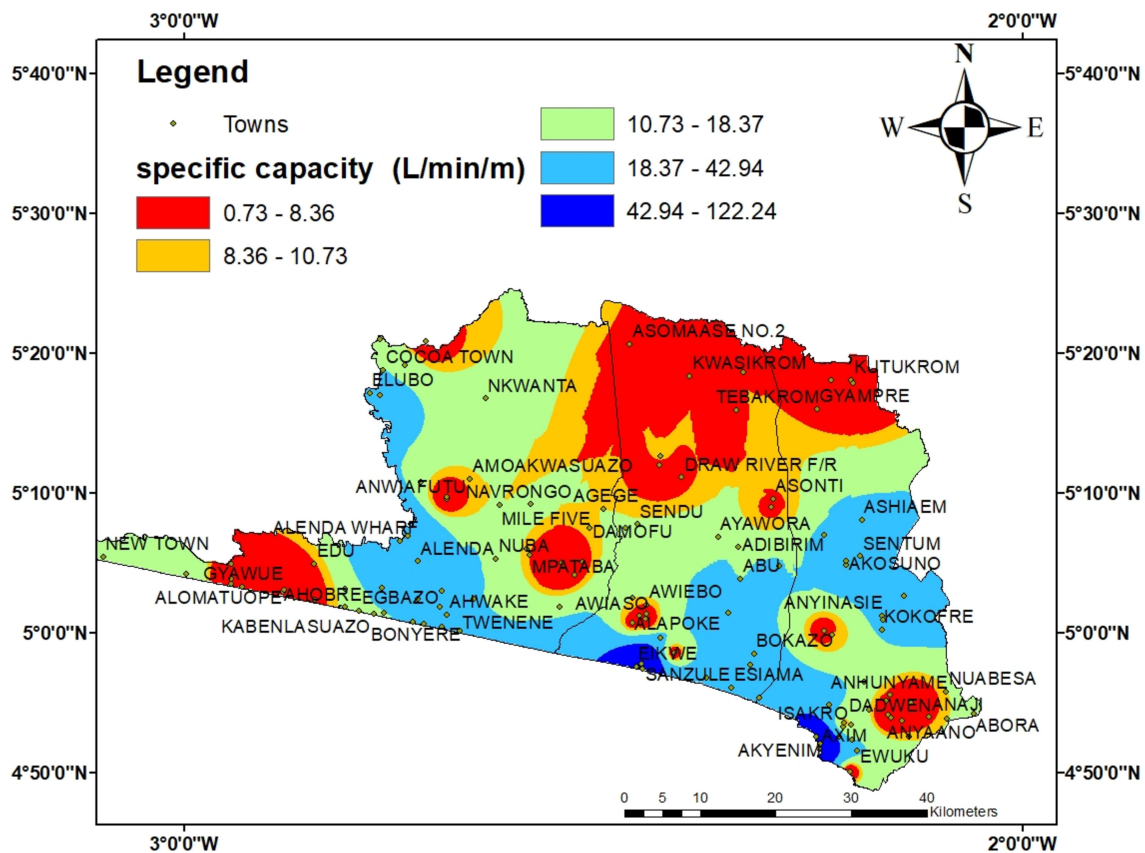


Fig. 7 Spatial distribution map of specific capacity for the study area

in groundwater. This mineral content cannot clog pore spaces, thereby increasing the hydraulic conductivity of the aquifer (Fig. 6) as discussed previously, making the pore spaces more easier for water to flow through the aquifers of the Apollonian formation and the Birimian supergroup of the Tano River Basin.

The electrical conductivity (EC) values of the borehole water had a mean of 237.60 S/cm and the overall data (Table 4), indicates low salt enrichment. However, none of the EC values met the WHO (2011) acceptable limit of 1500 μ S/cm for drinking water. The results of the above physical parameters are consistent with previous research conducted on existing groundwater in the same location (Edjah et al. 2019, 2021) and related geological formations in Cameroon (Nganje et al. 2019). Based on the above physical parameters, it can be concluded that the borehole water in the Tano River Basin is suitable for consumption, but attention should be given to the minimum proportion of the boreholes with pH levels below the WHO (2011) limit.

The borehole water analysis in the Tano River Basin revealed the presence of various cations and anions (Table 5). Calcium (Ca^{2+}) was the most represented cation, with levels ranging from 4 to 143 mg/L (Table 5). In one borehole developed in the rocks of the Birimian

Supergroup, Ca^{2+} content exceeded the WHO (2011) permissible limit of 75 mg/L for drinking water, and this is due to the slow weathering of silicate minerals (hornblende, feldspars, and plagioclase) in the underlying geology. Magnesium (Mg^{2+}) concentrations were below the WHO (2011) limit of 50 mg/L, except in the same borehole which had elevated calcium content, and this might be due to weathering of ferromagnesium minerals (biotite, hornblende, and mica), which also exist in the Birimian Supergroup rocks. Sodium (Na^+) content was within the WHO (2011) permissible limit of 200 mg/L in all boreholes. Potassium (K^+) was within WHO (2011) limits of 12 mg/L, except in two boreholes with high levels due to weathering of clay minerals in the underlying geology (Fig. 1) where these boreholes were drilled. The most abundant anion was bicarbonate (HCO_3^-), with levels within the WHO (2011) limit of 500 mg/L, and this is attributed to carbonate mineral dissolution and silicate mineral weathering (Gastmans et al. 2010), which exist in the underlying geology of the Tano River Basin (Fig. 1). Sulphate (SO_4^{2-}), chloride (Cl^-), and nitrate (NO_3^-) were all within WHO (2011) permissible limits (Table 5).

In summary, while the majority of borehole water samples conformed to WHO (2011) drinking water

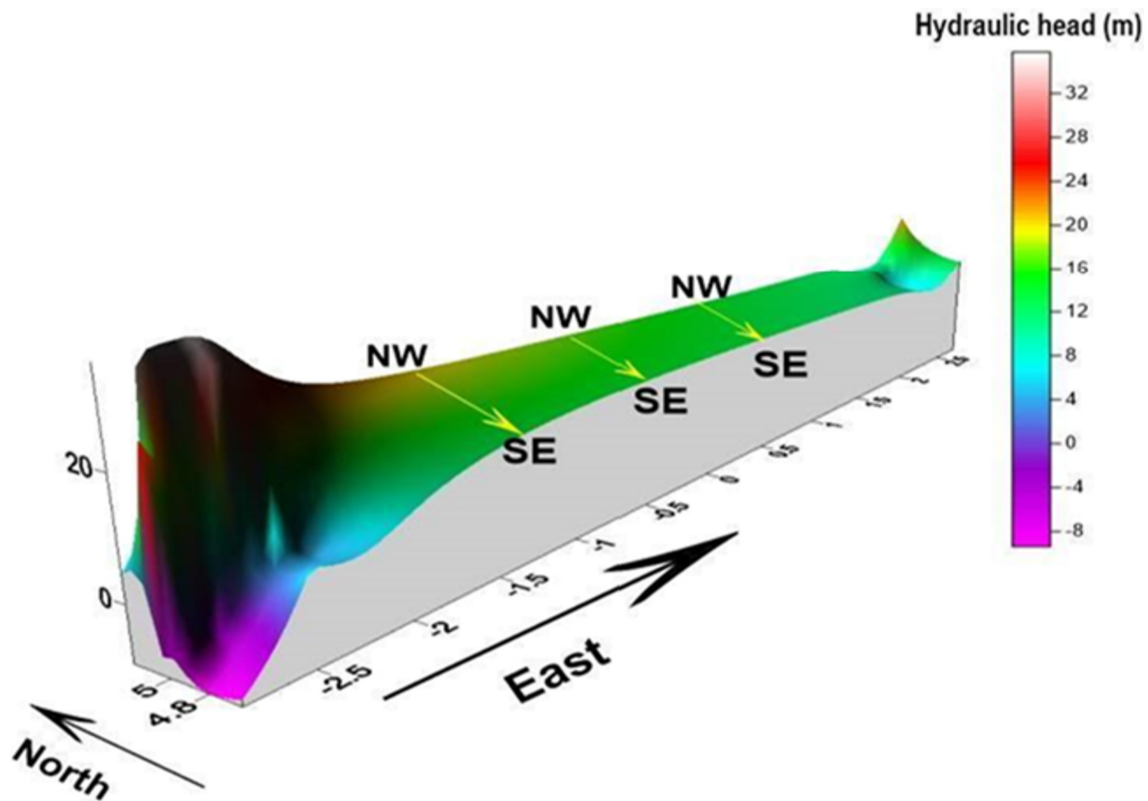


Fig. 8 Borehole contour map of the study area in 3 dimensions

standards for cations and anions, the occurrences of elevated calcium and potassium levels in some borehole water samples underscore the significant impact of underlying geological compositions on water quality, highlighting the need for targeted monitoring and management strategies in areas characterized by the rocks of the Apollonian formation and the Birimian supergroup.

Also under this section, a Pearson correlation matrix is used to examine the relationships between the field parameters, cations, and anions. The results are shown in Table 6 and remarkable correlations which are highlighted are seen among the variables. Notably from the Table 6, the good correlation between TDS and pH indicates a carbonate aquifer, stable geological settings, water–rock interaction, physicochemical influences such as oxidation reactions and hydrochemical processes (Subba 2002). The perfect correlation between TDS and EC reveals the suitability of the groundwater for all socio-economic uses since the study recorded low EC and TDS values in the sampled groundwater. The good correlation between TH and (pH, EC, TDS) shows that the geochemical interactions of the ions specifically calcium and magnesium may be influenced by the potential dissolution of carbonate and weathering of silicate minerals from the underlying geology likely leading to a karst aquifer even though the aquifers are unconfined to confined. In addition, the

aquifers where these boreholes were drilled may be likely influenced by sea water intrusion leading to the above correlation. Cl^- is a significant contributor to groundwater mineralization as it is a highly mobile anion (Subba 2002), leading to the moderate connection between Cl^- and (EC, TDS). In addition, geogenic and anthropogenic sources might influence the moderate correlation between Cl^- and (EC, TDS). The moderate relationship between Cl^- and TH are affected by natural geochemical processes occurring within the aquifers of the Tano River Basin, as well as anthropogenic influences. The perfect correlation between HCO_3^- and TH and the strong correlation between HCO_3^- and (pH, EC, and TDS) suggests that the groundwater in the Tano River Basin is significantly influenced by carbonate minerals (limestones) (Drever 1988), which exist in the underlying geology. It also indicates the potential for karst features in the Tano River Basin. Since gypsum or anhydrite are absent in the underlying geology, the moderate correlation between SO_4^{2-} and EC might be linked to redox conditions (oxidation–reduction) in the aquifers, and anthropogenic influences. The moderate correlation between Na^+ and pH suggests probable weathering of silicate minerals (such as hornblende, plagioclase, feldspar, etc.) from the underlying geology, water–rock interaction, anthropogenic sources etc. Further evidence that Na^+ is important in the mineralization of groundwater in the Tano

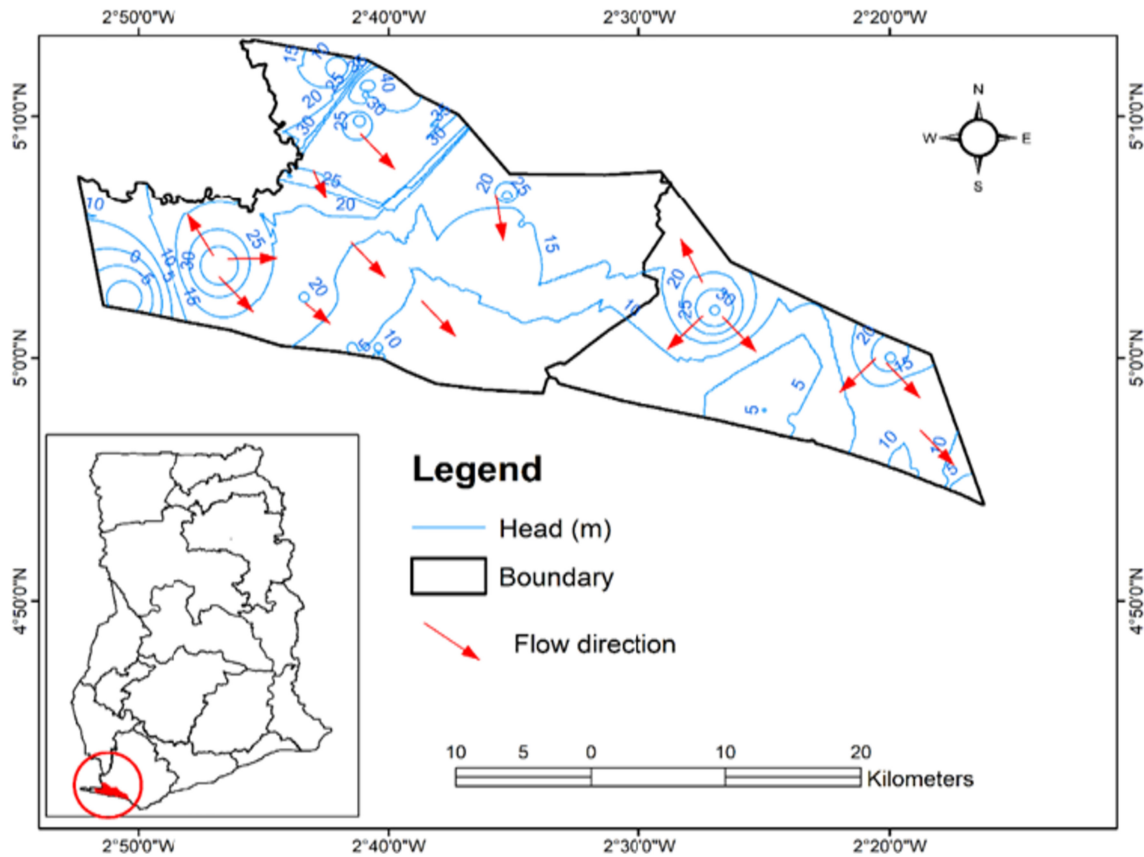


Fig. 9 An illustration of the borehole water’s flow direction in the research region

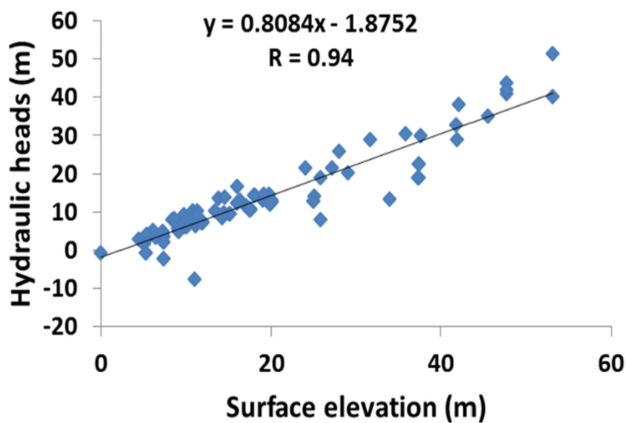


Fig. 10 An experiential connection between surface elevation and hydraulic heads

River basin comes from the perfect correlation between Na^+ and (EC and TDS). The perfect relationship between Na^+ and Cl^- reveals ion exchange processes, geochemical influences or seawater intrusion. The strong relationship between K^+ and pH points to the chemical weathering of silicate minerals (K-feldspars, biotite, mica etc.) from the underlying geology (Fig. 1), residence times of the groundwater, and the conditions of groundwater flow. The

Table 4 Descriptive statistics of the physical parameters of the drilled boreholes

Parameters	EC ($\mu\text{s}/\text{cm}$)	TDS (mg/L)	pH
Number of samples	55	55	55
Mean	237.60	114.11	6.69
Standard error	22.00	10.65	0.07
Median	212.00	106.50	6.91
Mode	219.00	108.00	6.99
Standard deviation	152.40	73.82	0.52
Sample variance	23226.77	5448.76	0.27
Kurtosis	28.12	24.39	1.65
Skewness	4.79	4.29	- 1.41
Minimum	101.00	34.20	5.20
Maximum	1150.00	542.20	7.70
Sum	11404.70	5477.10	321.02
Confidence level (95.0%)	44.25	21.43	0.15

strong correlation between K^+ and (EC and TDS) indicates that the presence of K^+ in groundwater of the study area is linked to the overall mineralogical composition of the aquifer. Additionally, the strong relationship between K^+

Table 5 The statistical analysis of hydrochemical parameters for the sampled borehole water in the research area

Parameters	Ca ²⁺ (mg/L)	Mg ²⁺ (mg/L)	TH (mg/L)	Na ⁺ (mg/L)	K ⁺ (mg/L)	HCO ₃ ⁻ (mg/L)	SO ₄ ²⁻ (mg/L)	NO ₃ ⁻ (mg/L)	Cl ⁻ (mg/L)
Number of samples	55	55	55	55	55	55	55	55	55
Mean	52.75	28.25	97.73	22.49	3.08	68.12	7.36	1.20	36.67
Standard Error	4.63	3.57	7.62	8.37	0.91	17.58	0.76	0.08	5.46
Median	56.00	23.00	89.00	14.00	1.80	31.72	6.86	1.09	26.65
Mode	15.00	23.00	37.00		1.10	197.64	10.00	1.09	5.50
Standard Deviation	32.06	24.76	52.77	35.51	3.85	74.60	5.26	0.42	37.84
Sample Variance	1027.55	613.28	2785.18	1261.15	14.86	5565.26	27.64	0.18	1431.82
Kurtosis	- 0.18	- 1.04	- 0.84	16.38	4.65	- 0.21	11.38	1.74	12.01
Skewness	0.25	0.55	0.42	3.97	2.24	1.25	2.59	1.37	2.88
Minimum	4.00	0.70	19.00	3.40	0.20	6.10	0.01	0.54	0.04
Maximum	143.00	79.00	205.00	162.00	14.60	208.62	33.00	2.31	224.00
Sum	2532.00	1356.10	4691.00	404.80	55.40	1226.10	353.06	34.83	1759.98
Confidence level (95.0%)	9.31	7.19	15.32	17.66	1.92	37.10	1.53	0.16	10.99

Table 6 Correlation matrix of the physicochemical parameters of the borehole water samples

	pH	EC	TDS	TH	Cl ⁻	HCO ₃ ⁻	SO ₄ ²⁻	Na ⁺	K ⁺	Ca ²⁺	Mg ²⁺	NO ₃ ⁻
pH	1.0											
EC	0.4	1.0										
TDS	0.5	1.0	1.0									
TH	0.6	0.6	0.6	1.0								
Cl ⁻	0.3	0.7	0.7	0.5	1.0							
HCO ₃ ⁻	0.8	0.7	0.7	1.0	0.4	1.0						
SO ₄ ²⁻	0.0	0.5	0.4	0.3	0.2	0.3	1.0					
Na ⁺	0.5	0.9	0.9	0.4	1.0	0.4	0.3	1.0				
K ⁺	0.6	0.7	0.7	0.3	0.8	0.3	0.5	0.8	1.0			
Ca ²⁺	0.7	0.1	0.3	0.8	0.2	0.9	0.1	0.1	0.1	1.0		
Mg ²⁺	0.5	0.1	0.2	0.7	0.4	0.6	0.0	0.8	0.6	0.8	1.0	
NO ₃ ⁻	0.3	0.1	0.1	0.3	0.0	0.1	- 0.2	0.1	0.1	0.2	0.3	1.0

With the exception of 25 °C, all parameters are in milligrams per litre (mg/L) and EC is in µS/cm

The bold shows the strong or perfect correlation between the variables

and Cl⁻ may be due to human activity such as the application of fertilisers by the coconut farmers in the study catchment or a common geochemical process. The moderate correlation between K⁺ and SO₄²⁻ might result from anthropogenic sources or ion exchange reactions, or geochemical influences. Furthermore, the strong correlation between K⁺ and Na⁺ suggests the possibility of cation—exchange processes or a common geochemical origin within the aquifer (Drever 1988) or weathering of feldspars and micas from the underlying geology or water–rock interactions or anthropogenic influences etc. The strong correlation between Ca²⁺ and pH indicates that water–rock interactions, particularly the dissolution of calcium-bearing minerals (e.g. hornblende) from the underlying geology,

have a significant influence on groundwater chemistry and pH levels. The strong correlation between Ca²⁺ and TH indicates calcium hardness in the borehole water or dissolution of carbonate minerals from the underlying geology or water–rock interactions. Further, the strong correlation between Ca²⁺ and HCO₃⁻ reveals the dissolution of limestones from the underlying geology or that the aquifers in the Tano River Basin are being recharged by extensive rainfall (Khashoggi and El Maghraby 2013). This is possible because the study area record high rainfall amounts in Ghana and studies conducted by Edjah et al. 2019 indicates the that the groundwater recharge in the study area is of meteoric origin.. The moderate correlation between Mg²⁺ and pH suggests that magnesium-bearing minerals (e.g.

dolomites, biotite, ferromagnesium minerals) from the underlying geology and water–rock interactions are significant contributors to the chemistry of groundwater in the study area. Magnesium hardness in the groundwater is also revealed by the strong correlation between Mg^{2+} and TH. Additionally, the strong relationship between Mg^{2+} and HCO_3^- suggests a potential location for recharge as well as the potential for carbonate mineral dissolution (Khashoggi and El Maghraby 2013) and weathering of silicate minerals (plagioclase, hornblende, etc.) (Gastmans et al. 2010) from the underlying geology. The likelihood of cation-exchange processes at the soil–water interfaces or weathering of silicate minerals (hornblende, plagioclase, feldspar, etc.) from the underlying geology is revealed by the strong relationship between Mg^{2+} and Na^+ (Gastmans et al. 2010). Furthermore, the chemical weathering of biotite and granitic rocks in the underlying geology is revealed by the strong relationship between Mg^{2+} and K^+ . Additionally, the strong correlation between Mg^{2+} and Ca^{2+} points to the dissolution of limestones as well as the weathering of hornblende and granitic rocks from the underlying geology.

4.2.1 Groundwater suitability for drinking purposes

4.2.1.1 Bacteriological parameters The data are normally distributed, as shown in Table 7 where the kurtosis and skewness were within $+7$ to -7 and $+2$ to -2 , respectively. In addition, the borehole water's *Escherichia coli* (*E. Coli*) content ranges from 101.40 MPN/100 mL to below the non-detect threshold (Table 7). *Escherichia coli* levels in 7 of the 55 boreholes that were drilled in areas

underlain by the rocks of the Apollonian Formation are greater than what WHO (2011) recommends. When increased *E. coli* values are found in drinking water, they constitute a major disease concern since they are potential pathogens, along with *Campylobacter coli*, *Vibrio cholerae*, *Campylobacter jejuni*, and *Yersinia enterocolitica* (WHO 2017). The total plate count ranged from the non-detection limit to 7380 MPN/CPU, while the total coliform concentration in the borehole water ranged from the non-detection limit to 2419.6 MPN/100 mL, as shown in Table 7. Both the total coliform and total plate counts are high in 18 ($n = 55$) of the boreholes, all of which were drilled and developed in regions covered by rocks of the Apollonian Formation. High organic loadings, untreated faecal pollution, and seawater intrusion may all be likely contributing factors to the high *E. coli* levels in 7 of the boreholes and the elevated coliform counts in 18 of the boreholes, respectively. In addition, the elevated coliform counts could be a result of storage runoff getting into the study area as a result of the significant flooding (<https://allafrica.com/stories/202207060262.html>), and leachate could be blamed for the high coliform loads. The underlying geology of the Tano River Basin have a high potential for infiltration and in a fractured aquifer with carbonate rocks, contamination of groundwater with microbiological loadings can be of particular concern. This is due to the fact that in such an aquifer, groundwater can flow relatively quickly (see Figs. 8, 9). Through a number of geochemical mechanisms, the increase in microbial activity in some of the boreholes especially those drilled and developed in areas underlain by the rocks of the

Table 7 Statistical summary of the microbiological loads in the borehole water with MPN/100 denotes coliform forming units per 100 mL of borehole water

Parameters	<i>E. coli</i> (MPN/100 mL)	Total coliform (MPN/100 mL)	Total plate count (MPN/100 mL)
Number of samples	55	55	55
Mean	15.89	881.90	4455.11
Standard error	7.77	215.72	684.95
Median	0.00	488.40	5650.00
Mode	0.00	1986.30	7380.00
Standard deviation	32.97	915.24	2905.98
Sample variance	1087.23	837662.80	8444748.58
Kurtosis	2.55	- 1.33	- 1.64
Skewness	2.00	0.65	- 0.50
Range	101.40	2417.60	6825.00
Minimum	0.00	2.00	555.00
Maximum	101.40	2419.60	7380.00
Sum	286.10	15874.20	80192.00
Confidence level (95.0%)	16.40	455.14	1445.11

Apollonian Formation may have an impact on the mobility of specific elements in the borehole water (Bowell et al. 1996). The results of this study, which is the first to examine the microbiological loadings in groundwater across the entire study area, are consistent with the results obtained by Armah (2014), who assessed groundwater quality in relation to bacterial load in a Ghanaian gold mining village. Ultimately, the above discussion has served as an important contribution to the understanding of groundwater quality with respect to microbiological loadings in the Tano River Basin and has provided valuable insights for informed decision-making and sustainable groundwater resource management practises.

4.2.1.2 Trace element This section discusses the trace element concentrations in groundwater from the various developed boreholes. The majority of the borehole water contains low median concentrations of 18 trace elements, all below the permissible values for drinking water according to WHO (2011) standards (Table 8). However, a few boreholes exhibit high concentrations of certain trace elements which will be explained further. The dominant trace element is iron (Fe), which suggests the presence of ferromagnesium minerals like biotite and sulphide-bearing minerals (pyrite, arsenopyrites, chalcopyrite, etc.), which exist in the underlying geology of the study area (Leube et al. 1990). Some boreholes show elevated levels of Fe, Cr, Al, Ni, Sr, As, and Pb, which exceed the WHO (2011) permissible limits of 0.3, 0.05, 0.2, 0.05, 0.015, 0.01, and 0.01 mg/L, respectively, for drinking water. These elements can be toxic (Bowell et al. 1996), with Al potentially linked to Alzheimer's disease (Martyn et al. 1989). The elevated trace elements might be associated with acidic borehole water (Smedley and Kinniburgh 2002), influenced by anthropogenic or microbial activities. Strontium (Sr) content is high in boreholes located in areas underlain by the rocks of the Apollonian formation. Extreme exposure to Sr may lead to health issues (Health Canada 2018). Saxena et al. (2004) suggested Sr values of < 1.6 mg/L for fresh groundwater, 1.6 to 5 mg/L for brackish water, and > 5 mg/L for saline groundwater in a coastal aquifer. Per Saxena et al.'s (2004) classification, all boreholes drilled and developed in the Tano River Basin are fresh (Sr < 1.6 mg/L). Arsenic (As) content is also notable in boreholes developed in areas underlain by the rocks of the Birimian supergroup. The Birimian Supergroup rocks in the Tano River Basin is known to contain various geological formations and mineral deposits like arsenopyrite (FeAsS₂). Previous geological studies conducted by Luebe et al. (1990) and Dzigbodi-Adjimah and Asamoah (2009) have identified arsenic as one of the trace elements hosted within sulphide minerals found in the rocks of the Birimian Supergroup. Their studies provided important geological

evidence of the presence of arsenic-bearing minerals in the upper part of the study region (Fig. 1). Hence, when sulphide minerals like arsenopyrite are exposed to oxygen (O₂) and water (H₂O), they undergo a process known as sulphide mineral oxidation. This process leads to the chemical transformation of these minerals and the release of their constituent elements, including arsenic. During sulphide mineral oxidation, arsenic is released from the arsenopyrite mineral. The chemical reactions involved in this process can convert arsenic into soluble forms, such as arsenate (H₂AsO₄⁻) or arsenite (H₃AsO₃⁻), which can then be mobilized into the groundwater. The mobilized arsenic can likely contaminate the aquifer, resulting in elevated arsenic levels in the sampled borehole water that tap into the aquifer of the Birimian supergroup of the Tano River Basin. The elevated arsenic concentrations in the borehole water can have significant health implications, as long-term exposure to high levels of arsenic is associated with various health risks, including cancer and other health disorders (Edmunds and Smedley 1996). Lead (Pb) concentrations are higher in boreholes located in areas underlain by the rocks of the Apollonian formation. This is likely due to groundwater recharge from surface water in contact with sulphide minerals. In the study area, Dzigbodi-Adjimah and Asamoah (2009) discovered Pb as one of the trace elements hosted by sulphide minerals in the underlying geology of the study area. High levels of Pb can cause various health problems (WHO 2011). Nickel (Ni) concentrations are high in boreholes related to the rocks of the Apollonian Formations, suggesting surface water recharge from contact with sulphide minerals. Luebe et al. (1990) discovered Ni, As, Zn, Pb, etc. as host elements in sulphide minerals in the underlying geology of the study area. Human exposure to nickel can lead to health issues.

4.2.1.3 Determination of the overall suitability of borehole water for drinking using WQI (water quality index) The Tano River Basin's groundwater's suitability for drinking is assessed using the drinking water quality standards recommended by WHO (2011). Based on the field parameters, cations, anions, and trace elements, the water quality index is calculated. The following is a representation of the water quality index (WQI) equation (Magesh et al. 2013), utilised in this study:

$$WQI = \sum Sli \quad (8)$$

$$Sli = Wi \times qi \quad (9)$$

$$qi = \left(\frac{ci}{si} \right) \times 100 \quad (10)$$

$$Wi = \frac{wi}{\sum_{i=1}^n wi} \quad (11)$$

Table 8 Descriptive statistics of trace element parameters in the drilled boreholes (all parameters are measured in mg/L) and BDL is below the detection limit ((0.001))

Parameters	Cu	Mn	Fe	As	Al	Zn	B	Ba	Cd	Cr	Co	Pb	Ni	Sc	Ag	Sr	Ti	V
WHO (2011) Standards	2	0.4	0.3	0.01	0.3	5	0.5	0.7	0.003	0.05	0.05	0.01	0.02	0.04	0.05	0.02	0.1	3
Number of samples	55	55	55	55	55	55	55	55	55	55	55	55	55	55	55	55	55	55
Mean	0.008	0.039	0.284	0.003	0.140	0.029	0.06	0.014	0.0002	0.004	0.002	0.025	0.006	0.011	0.0005	0.146	0.007	0.004
Standard error	0.005	0.008	0.109	0.002	0.069	0.005	0.03	0.002	7.82E-05	0.001	0.001	0.006	0.003	0.001	0.0002	0.037	0.002	0.001
Median	0.000	0.016	0.090	0.000	0.010	0.010	0.03	0.011	0	0.002	0.001	0.000	0.003	0.010	0.0005	0.082	0.004	0.001
Mode	0.000	0.000	0.000	0.000	0.000	0.000	0.02	0.005	0	0.002	0.000	0.000	0.002	0.010	0.0005	0.006	0.006	0.003
Standard deviation	0.038	0.058	0.754	0.014	0.474	0.034	0.10	0.009	0.00033	0.005	0.004	0.043	0.011	0.003	0.0004	0.155	0.010	0.006
Sample variance	0.001	0.003	0.568	0.000	0.224	0.001	0.01	0.000	1.10E-07	2.21E-05	1.7E-05	0.002	0.000	0.000	0.0000	0.024	0.000	0.000
Kurtosis	38.268	5.162	34.266	33.824	39.945	-1.421	14.54	0.992	-7.36E-01	8.82E+00	2.119	2.024	8.576	13.000	-1.7486	0.956	16.325	10.610
Skewness	6.019	2.138	5.595	5.667	6.132	0.570	3.79	1.246	1.121	2.792	1.825	1.740	2.910	3.606	0.1325	1.531	3.966	3.124
Range	0.250	0.270	5.000	0.087	3.200	0.090	0.39	0.031	0.001	0.020	0.013	0.150	0.045	0.010	0.0009	0.459	0.046	0.024
Minimum	BDL	BDL	BDL	BDL	BDL	BDL	0.02	0.005	BDL	BDL	BDL	BDL	BDL	0.010	BDL	0.016	0.002	0.001
Maximum	0.250	0.270	5.000	0.087	3.200	0.090	0.41	0.036	0.001	0.020	0.013	0.150	0.045	0.020	0.0010	0.475	0.048	0.025
Sum	0.400	1.859	13.640	0.149	6.560	1.345	0.84	0.259	0.004	0.067	0.044	1.221	0.115	0.140	0.0031	2.619	0.125	0.065
Confidence level (95.0%)	0.011	0.017	0.219	0.004	0.139	0.010	0.05	0.005	0.0002	0.002	0.002	0.012	0.006	0.002	0.0004	0.077	0.005	0.003

Table 9 The assigned weights and relative weights of trace elements

Trace elements (mg/L)	WHO (2011) Permissible Standards for drinking water	Weight (wi)	Relative weight (Wi)
Cr	0.05	5	0.23
Mn	0.4	4	0.18
Fe	0.3	4	0.18
Co	0.05	1	0.05
Ni	0.006	1	0.05
Cu	0.05	2	0.09
Zn	5	1	0.05
As	0.01	5	0.23
Cd	0.003	5	0.23
Pb	0.01	5	0.23
Al	0.2	2	0.09
		$\sum wi = 72$	$\sum Wi = 3.02$

Tables 9, 10, 11 shows both the computed relative weights and the weights given to each parameter. In order to evaluate the various levels of water quality at each drilling location for drinking purposes, including excellent (WQI < 50), good (50 < WQI < 100), fair (100 < WQI < 200), bad (200 < WQI < 300), and extremely poor (WQI > 300), Fig. 11 shows the water quality index map developed using ArcGIS 10.5 software. The Water quality index map of the study region (Fig. 11) indicates that boreholes drilled and developed in the northern, north western, north eastern along with few developed in the middle, southern, south eastern and south western yields excellent water and excellent to good water for drinking, respectively. Also, boreholes drilled in the eastern, southwestern, north eastern, middle and southwestern zone of the study area along with few drilled in the southern zone yields good to fair water for drinking. Furthermore, boreholes drilled in the middle, southern and south western zone of the study area, gave out fair to poor water for drinking. Additionally, drinking water quality was low to extremely bad from boreholes that were drilled in the southern region of the research area. Further to the map (Fig. 11), it can be seen that the boreholes drilled in the coastal zone of the study area where they are underlain by the rocks of the Apollonian formation have quality issues. This is probably due to the high porosity and permeability rocks of the Apollonian formation (Kesse 1985; Fig. 6). This feature could facilitate groundwater contamination in the Tano River Basin due to greater volume of pore space available to store groundwater. This negatively affect the groundwater quality in these areas.

4.2.1.4 Unsupervised machine learning technique This study uses unsupervised machine learning algorithms (k-

Table 10 The assigned weights and relative weights of chemical parameters

Chemical Parameters	WHO standards (2011)	Weight (wi)	Relative weight (Wi)
pH (on scale)	6.5–8.5	4	0.18
EC ($\mu\text{S}/\text{cm}$)	500	4	0.18
TDS (mg/L)	500	4	0.18
Ca^{2+} (mg/L)	75	2	0.09
Mg^{2+} (mg/L)	50	2	0.05
TH (mg/L)	500	2	0.09
HCO_3^- (mg/L)	500	3	0.14
SO_4^{2-} (mg/L)	250	4	0.18
NO_3^- (m/L)	50	5	
Cl^- (mg/L)	250	3	0.14
Na^+ (mg/L)	200	2	0.09
K^+ (mg/L)	12	2	0.09

Table 11 Water quality index results and water types of the samples

Samples	WQI values	Classification	Samples	WQI values	Classification
BH1	32.48	Excellent	BH25	24.03	Excellent
BH2	57.67	Good	BH26	28.87	Excellent
BH3	50.31	Good	BH27	31.54	Excellent
BH4	36.33	Excellent	BH28	59.69	Good
BH5	31.73	Excellent	BH29	35.07	Excellent
BH6	44.61	Excellent	BH30	26.34	Excellent
BH7	56.00	Good	BH31	248.68	Poor
BH8	38.15	Excellent	BH32	96.43	Good
BH9	104.62	Fair	BH33	285.08	Poor
BH10	23.15	Excellent	BH34	296.46	Poor
BH11	26.19	Excellent	BH35	161.78	Fair
BH12	21.80	Excellent	BH36	111.39	Fair
BH13	37.32	Excellent	BH37	264.73	Poor
BH14	39.07	Excellent	BH38	242.92	Poor
BH15	24.24	Excellent	BH39	154.37	Fair
BH16	52.05	Good	BH40	134.57	Fair
BH17	33.18	Excellent	BH41	133.43	Fair
BH18	33.37	Excellent	BH42	229.26	Poor
BH19	39.81	Excellent	BH43	174.34	Fair
BH20	26.98	Excellent	BH44	62.22	Good
BH21	47.90	Excellent	BH45	171.70	Fair
BH22	28.95	Excellent	BH46	234.71	Poor
BH23	40.15	Excellent	BH47	378.50	Very poor
BH24	66.51	Good	BH48	95.22	Good

means clustering) to classify the groundwater in the study region based on the estimated aquifer hydraulic parameters, results of the physical parameters, cations, anions, microbiological loadings, and trace elements. Results obtained from the K-mean algorithms are compared using the silhouette method (Figs. 12, 13), with Table 12 showing the outcome. The silhouette coefficient assesses cluster quality and distance, with + 1 indicating well-positioned data, 0 indicating close proximity, and – 1 indicating incorrect

cluster position. With + 1 being the best and – 1 being the worst, clustering uses the K-mean technique to evaluate the average silhouette score. The study makes use of four clusters of overlapping data points (Fig. 14), and the highest loadings of an all-inclusive parameters as stated above were found in twenty boreholes located in the Apollonian Formation aquifer (Table 13). With the use of principal component analysis (PCA), the fitted K-model is evaluated (Fig. 14). Two primary loadings are present in

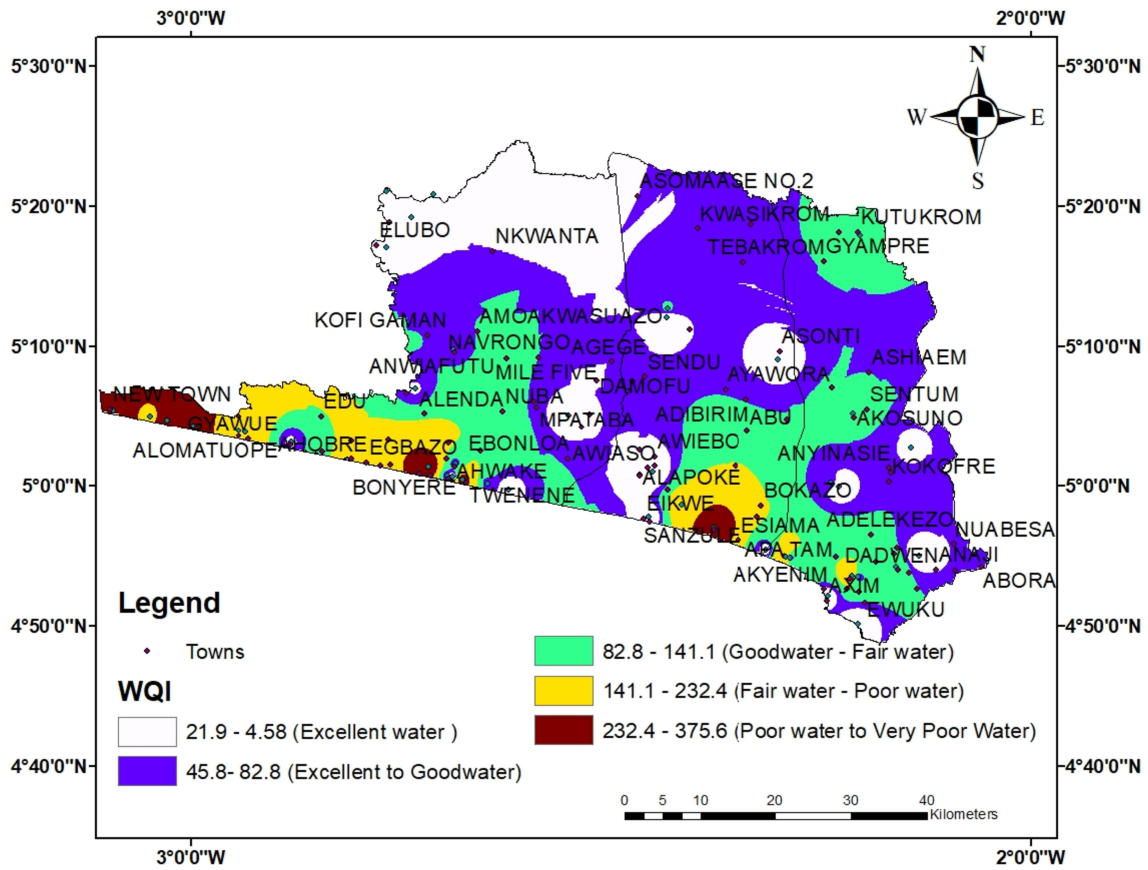
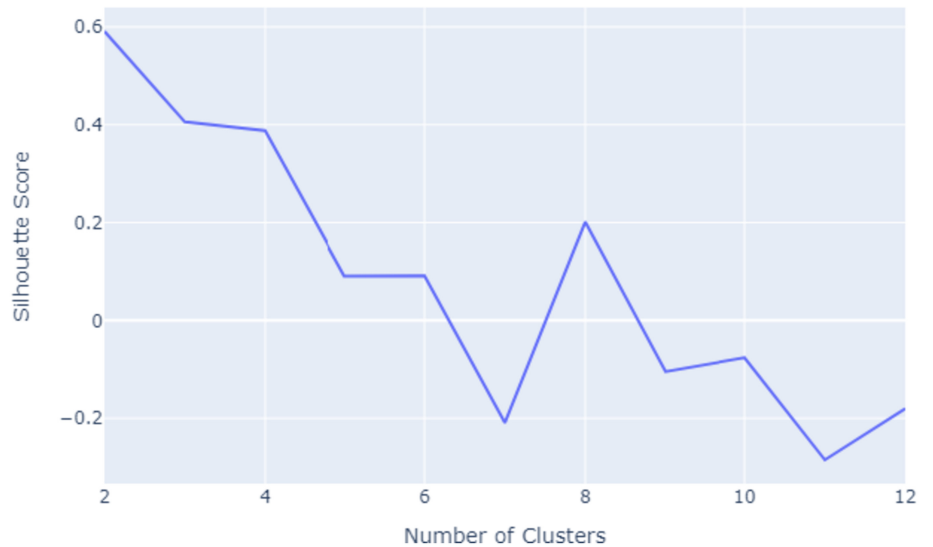


Fig. 11 Shows a spatial distribution map for the study area’s water quality index

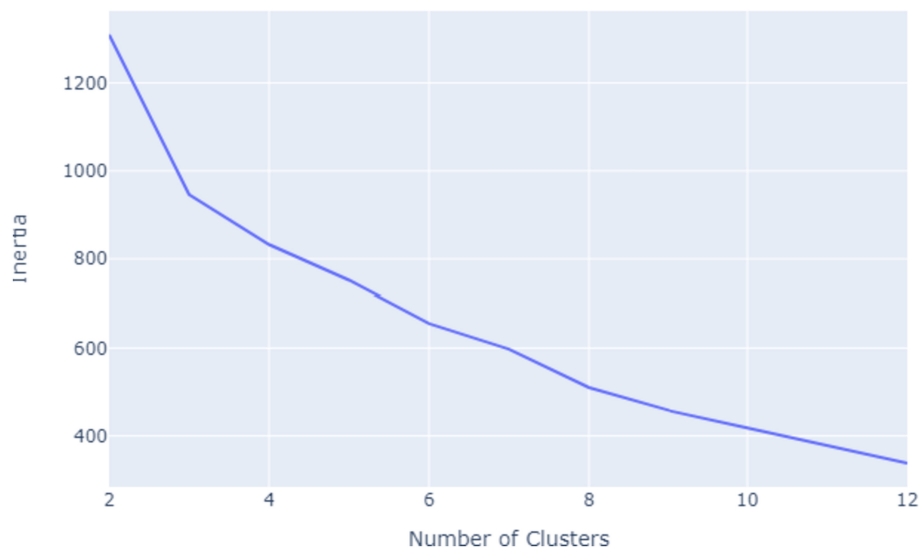
Fig. 12 Optimized Statistics Chart for K- means algorithm

K-Means Model: Silhouette Score vs Number of Clusters



the data set: the second-dominant in six boreholes in cluster 3 and the lowest in three boreholes in cluster 2 (Table 13). Clusters 0 and 1 have the largest and lowest loadings, respectively. In terms of quantity and quality using the

K-means algorithm, it can be seen that boreholes drilled in the aquifer of the Apollonian formation of the Tano River Basin account for the highest groundwater with similar characteristics.

Fig. 13 Optimized Statistics Chart for K mean algorithm**K-Means Model: Inertia vs Number of Clusters****Table 12** Silhouette and inertia scores for the borehole data set

Column1	Silhouette scores	Inertia_errors
0	0.590872345	1309.994795
1	0.405931329	946.1520136
2	0.388172485	832.4460253
3	0.090831684	751.5011473
4	0.091249141	655.5834043
5	-0.209085049	597.6684146
6	0.201500504	510.2191438
7	-0.104732655	458.1976387
8	-0.076043382	418.4900226
9	-0.284849075	378.0220061
10	-0.180273544	338.045292

4.3 Factors controlling the groundwater chemistry

The Piper (1944) diagram has been extensively used to illustrate groundwater classification and trends in hydro-geochemistry. In this study, the groundwater classification is shown in Fig. 15, which shows that the sampled borehole water has a dominant hydrochemical facies of Ca–HCO₃ type of water. Out of the 55 drilled boreholes, six boreholes exhibit the Na–Cl type of water, fourteen boreholes belong to the Ca–SO₄²⁻ type of water, ten boreholes belong to the mixed Ca–Mg–Cl type of water, and twenty-five boreholes belong to the Ca–HCO₃⁻ water type.

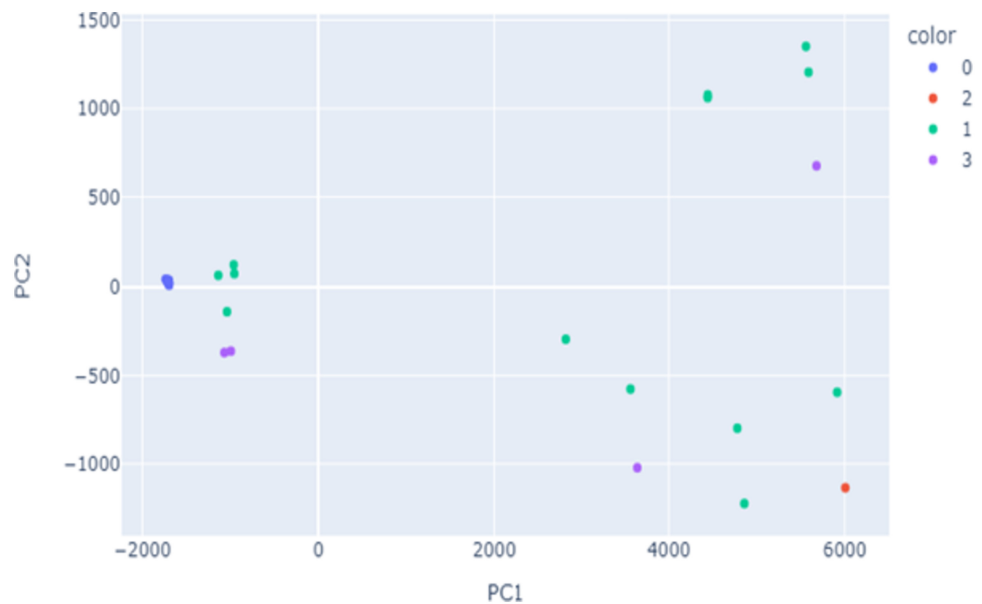
The Ca–HCO₃ water types suggest that the dissolution of carbonate minerals in the underlying geology likely results in active groundwater recharging areas (Appelo and

Postma 2005). Consequently, the geological formations (Rocks of the Apollonian) in these zones are favourable to water infiltration and percolation. Additional research by Edjah et al. (2015, 2019) suggests that the groundwater recharge in the study area is of meteoric origin, which is consistent with the identified recharge zones (Fig. 7) and supports the assertion made above.

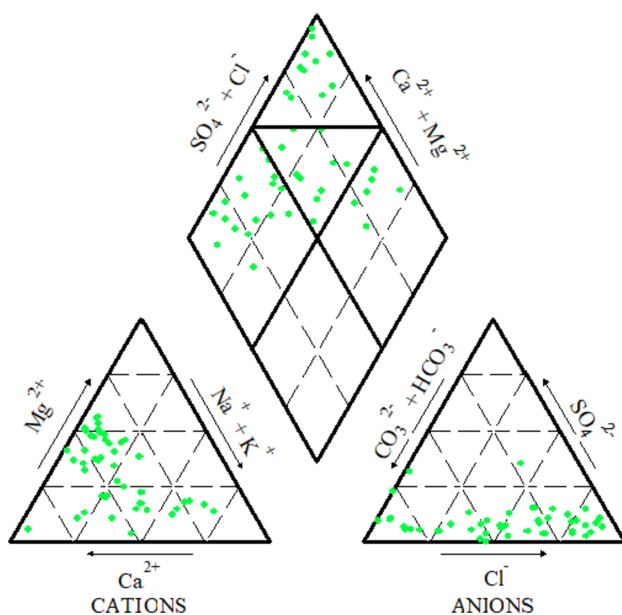
The boreholes clustering in the Na–Cl zone of the Piper (1944) diagram were all drilled in the aquifer of the Apollonian formation, and this is indicative of high sodium (Na⁺) and high chloride (Cl⁻). This chemical composition is a characteristic of seawater intrusion or ion exchange processes, which suggest their occurrence in the aquifer. It might be seawater intrusion due to the proximity to the sea and the high porosity and permeability of the unconsolidated rocks of the Apollonian formation. It can also be an ion exchange process due to the dissolution of carbonate minerals (limestones) from the rocks of the Apollonian formation.

The Ca–SO₄²⁻ reveals contaminated borehole water since gypsum is absent in the underlying geology of the study area.

The Ca–Mg–Cl water type frequently denotes the impact of carbonate mineral dissolution (calcium and magnesium) in limestones which exist in the underlying geology, as well as the potential for groundwater interaction with chloride-bearing sources. An occurrence of a karst aquifer in the Tano River Basin is also conceivable. This is due to the possibility of high groundwater concentrations of calcium and magnesium in a karst landscape (Appelo and Postma 2005), but further investigations are required.

Fig. 14 PCA representation of Clusters**Table 13** Total number of boreholes for each cluster for K-means algorithm

Cluster Number	K-means			K-means		
	Total number of boreholes	Percent (%)	Rock formations	Total number of boreholes	Percent (%)	Rock formations
0	10	18.2	Apollonian	20	36.36	Birimian
1	10	18.2	Apollonian	6	10.91	Birimian
2	3	5.45	Apollonian	0	0	Birimian
3	6	10.91	Apollonian	0	0	Birimian

**Fig. 15** Piper (1944) diagram used in classifying the boreholes of the study areas

Comparing Fig. 9 with Fig. 15, it is observed that the predominance of the CaHCO_3 water type could be linked to the lithology of the aquifers. This is because as groundwater flows from northward to southward (Fig. 9), it interacts with more carbonate (limestone) formations, thereby enhancing the dissolution of Ca^{2+} and HCO_3^- , which enriches the chemistry of the groundwater. This therefore suggests that the hydrogeological conditions of the Tano River Basin and the underlying geology likely influence the chemistry of the groundwater.

The aforesaid hydrochemical processes are further explained in this study using bivariate plots, which are shown in Figs. 16a–d. The majority of the borehole water samples fall over the 1:1 equiline, with a few falling below it, as seen in Fig. 16a, where the plot of $\text{Ca}^{2+} + \text{Mg}^{2+}$ versus Cl^- demonstrates an ion exchange process involving Ca^{2+} , Mg^{2+} and Na^+ ions (Belkhir et al. 2012). As groundwater flows through the aquifer of the Apollonian formation and the Birimian supergroup which contains limestones and silicate minerals (Biotite), respectively, they encounter minerals containing Ca^{2+} and Mg^{2+} which likely releases into the groundwater through dissolution. At the same time, the groundwater might come into contact

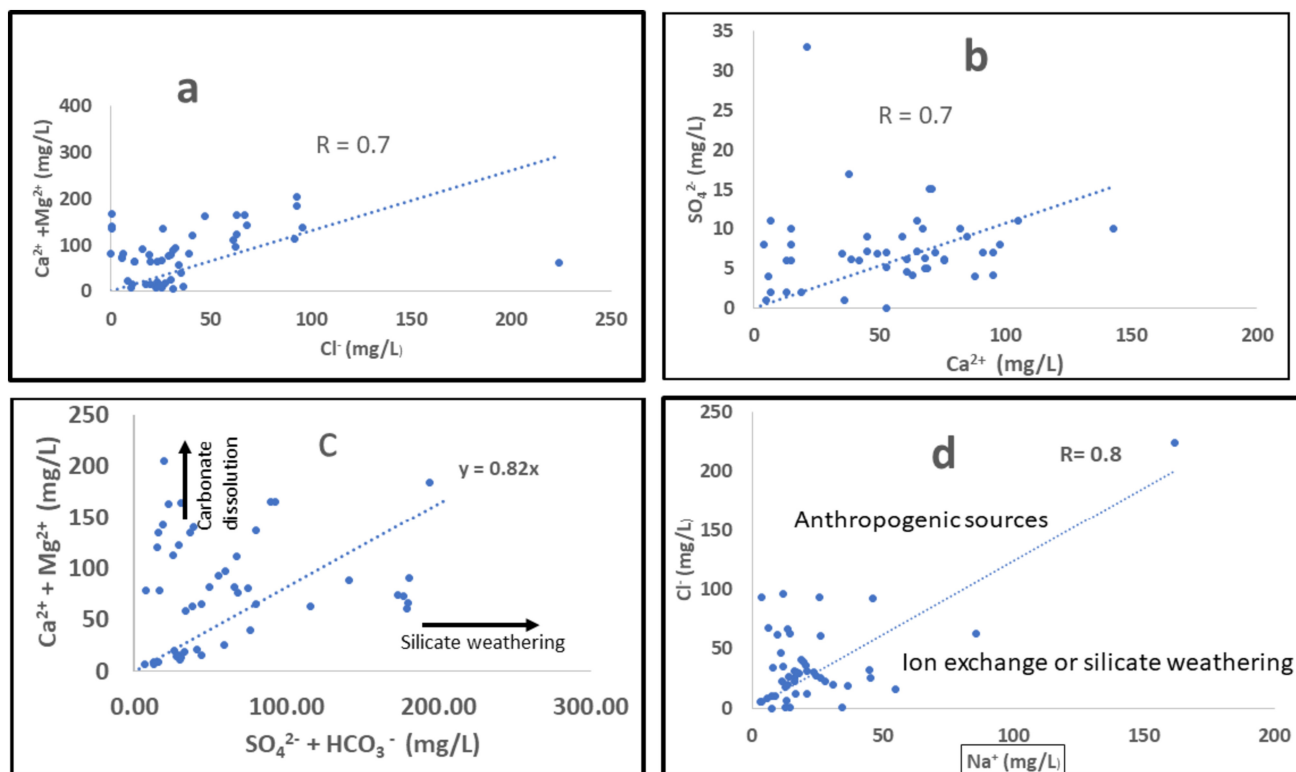


Fig. 16 Bivariate plots of **a** ($\text{Ca}^{2+} + \text{Mg}^{2+}$) against Cl^- , **b** SO_4^{2-} against Ca^{2+} , **c** ($\text{Ca}^{2+} + \text{Mg}^{2+}$) against ($\text{SO}_4^{2-} + \text{HCO}_3^-$), **d** Cl^- against Na^+

with solid phase materials that contains exchangeable ions. In addition, Fig. 16a reveal a strong correlation between $\text{Ca}^{2+} + \text{Mg}^{2+}$ and Cl^- which explains the above prevalence.

As can be seen in Fig. 16b, the majority of the borehole water samples are above the 1:1 equiline, while a small number are below and fewer cluster along the equiline. Additionally, the figure (Fig. 16b) displays a strong correlation, suggesting possible groundwater contamination which requires further investigations to identify the exact sources and nature of contamination. To further explain the occurrence of carbonate dissolution or silicate mineral weathering, a plot of $\text{Ca}^{2+} + \text{Mg}^{2+}$ versus $\text{SO}_4^{2-} + \text{HCO}_3^-$ is employed (Fig. 16c). According to Elango and Kannan (2007), the dominance of $\text{Ca}^{2+} + \text{Mg}^{2+}$ is a sign of carbonate dissolution and the abundance of $\text{SO}_4^{2-} + \text{HCO}_3^-$ over $\text{Ca}^{2+} + \text{Mg}^{2+}$ is a sign of silicate weathering. In this study, the majority of the boreholes show an abundance of $\text{Ca}^{2+} + \text{Mg}^{2+}$ over $\text{SO}_4^{2-} + \text{HCO}_3^-$. As can be observed in Fig. 16d, Cl^- dominates over Na^+ , suggesting anthropogenic sources or seawater intrusion as the cause of the chloride concentrations in the borehole water. Additionally, Na^+ ion exchange activities are related to the potential Na^+ deficiency in Fig. 16d (Belkhirri et al. 2012). Generally, this part of the study has provided valuable insights into the hydrochemical

processes controlling the groundwater chemistry in the Tano River Basin. The understanding of these processes is essential for effective groundwater management and protection, as well as for addressing potential issues related to groundwater quality and sustainability. However, it is essential to continue monitor and further investigate the above identified trends and correlations in order to develop a comprehensive groundwater resource management strategy and ensure the availability of safe and sustainable groundwater.

Further investigations are aided by the use of principal component analysis (PCA), which is computed using physical parameters, cations, anions, and trace elements. The Kaiser criterion (Kaiser 1960) is used to calculate the total number of significant principal components, and only principal components with eigenvalues greater than or equal to 1 are retained as potential sources of variation in the data set. Table 14 displays each principal component's variance expression as well as its relative relevance to the other principal components. From Table 14, PC1 represents 34.16% of the variance of the data set, and that is attributed to a strong positive correlation with EC, Cu, Pb, Zn, Na, K, HCO_3^- , and a strong negative correlation with Ca^{2+} , Mg^{2+} , NO_3^- , CO, and Cd. Groundwater with high PC1 loading is likely from the underlying geology which contains sulphide minerals (Ni, Pb and Zn) or effluents from

Table 14 Principal components, Eigen values and total variance for the quality of the borehole water

	PC1	PC2	PC3	PC4	PC5	PC6
pH	– 0.32	0.79	– 0.20	– 0.01	– 0.03	– 0.09
EC	0.59	0.78	0.03	0.10	– 0.10	– 0.04
TDS	0.44	0.85	0.08	0.11	– 0.13	– 0.07
TH	– 0.09	0.73	– 0.18	0.58	– 0.03	0.07
Cl [–]	0.25	0.72	0.28	– 0.07	– 0.08	0.14
Cu	0.63	0.65	0.14	– 0.37	– 0.01	– 0.01
Mn	0.31	0.07	– 0.26	0.60	0.26	– 0.11
Fe	0.32	– 0.25	0.78	0.35	0.06	– 0.07
SO ₄ ^{2–}	0.37	0.27	0.06	0.31	0.22	0.08
Cr	– 0.07	0.04	0.14	– 0.12	0.06	0.70
Pb	0.69	– 0.40	– 0.29	– 0.07	0.08	0.16
Ca ²⁺	– 0.60	0.59	– 0.10	0.38	– 0.01	0.01
Mg ²⁺	– 0.61	0.55	0.07	0.22	0.12	0.20
NO ₃ [–]	– 0.78	0.41	0.07	– 0.03	0.08	0.23
As	0.49	0.21	– 0.08	– 0.37	0.62	– 0.01
Al	0.28	– 0.36	0.83	0.21	0.09	– 0.03
P	– 0.42	0.28	0.06	0.18	0.15	0.60
Zn	0.86	– 0.42	– 0.03	0.13	0.07	0.06
Na ⁺	0.79	0.50	0.19	– 0.23	– 0.10	0.04
K ⁺	0.83	0.34	0.05	– 0.25	0.29	0.04
HCO ₃ [–]	0.74	0.24	– 0.24	0.45	– 0.15	– 0.02
Co	– 0.52	0.71	– 0.04	– 0.02	0.36	– 0.17
Cd	– 0.88	0.42	0.06	– 0.09	0.04	– 0.12
Ni	0.21	0.91	0.02	0.03	– 0.04	– 0.13
Eigen value	10.59	8.22	2.71	2.25	1.57	1.16
Variability %	34.16	26.52	8.74	7.26	5.07	3.74
Cumulative %	34.16	60.68	69.42	76.68	81.74	85.48

The bold shows the strong or perfect correlation between the variables

the oil and gas, and mining industries. Also, ion exchange processes (Na⁺ and K⁺) or anthropogenic sources and HCO₃[–] enrichment could likely influence the high PC1 loadings. PC2 (26.52%) as shown in Table 15 combines pH, EC, TDS, TH, Cl, Cu, Ca²⁺, Mg²⁺, Na⁺, Co, and Ni due to the strong positive relationship between PC 2 and the above-mentioned variables. This indicates high mineral composition (Ca²⁺ and Mg²⁺), with moderate EC and pH. PC 3 exhibits a strong correlation with Fe and Al and accounts for 8.74% of the variable in water quality. This is likely attributed to the geological influences or anthropogenic sources.

PC 4 shows an excellent connection with TH and Mn by taking 7.26% of the variance in water quality suggesting geological factors influencing the chemistry of the groundwater. PC 5 accounts for 5.07% of the fluctuation in water quality, which shows a strong relationship with As which might be of health concern. PC 6 shows a strong association with Cr and P and accounts for 3.74% of the variance in water quality which could originate from anthropogenic sources or natural mineral dissolution.

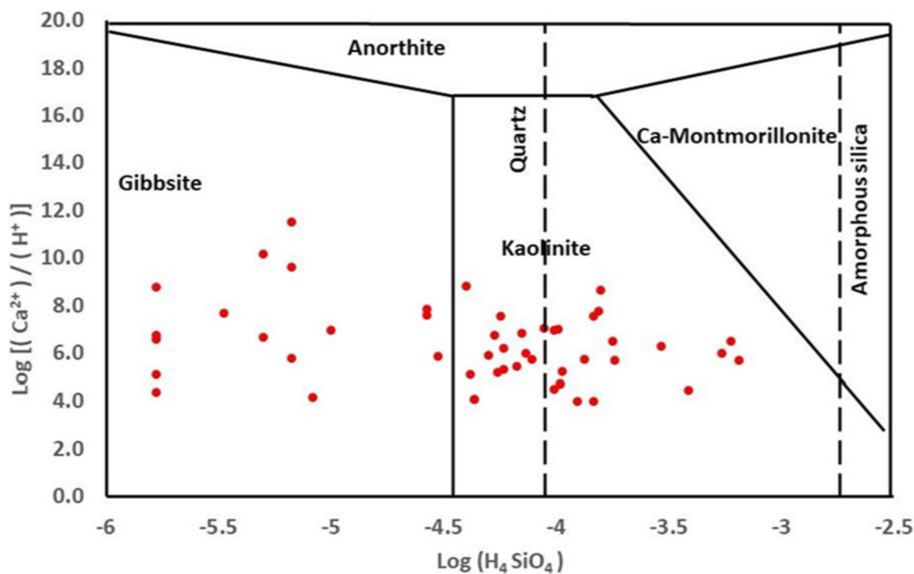
Geogenic processes, which are in conformity with the underlying geology and have fewer anthropogenic origins, are one of the potential factors regulating the chemical quality of the groundwater chemistry in the Tano River Basin, according to the information shown above. In conclusion, the integration of PCA in this study and its interpretation have enhanced the understanding of complex relationships controlling the groundwater chemistry in the Tano River Basin. By recognising the predominant influence of geogenic processes, groundwater resources can be better protected and sustained for both current and future uses.

The study employs a mineral stability diagram (Fig. 17) to better understand the chemistry of groundwater in the Tano River Basin. The underlying geology in the study region contains different clay minerals. The diagram reveals that 42 boreholes fall within the Kaolinite stability field (Fig. 17). This suggests that the borehole water in these areas has experienced a dilution of calcium ions and indicates the presence of kaolinite. Kaolinite has a low cation-exchange capacity (1–15 meq/100 g) (Appelo &

Table 15 Hazard quotients of all trace elements and cancer risks of Pb, Cr, and Cd in the study catchment

Elements	C _{water}	EXP _{ing}	EXP _{derm}	RfD _{ing}	RfD _{derm}	HQ _{derm}	HQ _{ing}	HI = HQ _{ing} + HQ _{derm}
As	0.003	0.000	0.005					0
Ba	0.014	0.001	0.008	70	14	0.001	1.18E−05	0.001
B	0.05	0.003	0.029					
Cd	0.0002	0.000	0.000	0.5	0	0.024	2.47E−05	0.02
Cr	0.006	0.000	0.007	3	0	0.463	1.18E−04	0.46
Co	0.0024	0.000	0.001	0.3	0	0.185	4.71E−04	0.19
Cu	0.0083	0.000	0.005	40	12	0.000	1.22E−05	0.00041
Pb	0.025	0.001	0.014	1.4	0.4	0.034	1.05E−03	0.04
Mn	0.04	0.002	0.023	5	0.8	0.029	4.71E−04	0.03
Ni	0.006	0.000	0.007	20	5.4	0.001	1.76E−05	0.001
Se	0.008	0.000	0.005	5	2.2	0.002	9.41E−05	0.002
Ag	0.0002	0.000	0.000					
Sr	0.15	0.009	0.087					
Ti	0.007	0.000	0.004					
V	0.004	0.000	0.002					
Zn	0.03	0.002	0.010	300	60	0.0002	5.88E−06	0.0002
Al	0.14	0.008	0.081					
Fe	0.28	0.016	0.162	300	45	0.004	5.49E−05	0.04

Fig. 17 Mineral Stability diagram for the CaO–H₂O–SiO₂–Al₂O₃ system in groundwater developed in the study area



Postma 2005), which promotes ion exchange processes in the groundwater. On the other hand, the remaining 13 boreholes lie in the Gibbsite stability field. This implies that as kaolinite forms in these areas, the pH of the borehole water is reduced, leading to more acidic conditions (Belkhiri et al. 2010). The presence of Gibbsite indicates a different chemical environment in these boreholes compared to those in the Kaolinite stability field. Also, the flow of groundwater in the Tano River Basin appears to be

unrestricted. This means that groundwater movement is not hindered or obstructed significantly. One possible reason for this unrestricted flow could be the unconsolidated rocks in the area where the boreholes were drilled. Unconsolidated rocks are loose and allow water to flow more easily compared to consolidated rocks. Additionally, incongruent mineral dissolution might be another factor influencing the chemistry of groundwater in the Tano River Basin. Incongruent mineral dissolution refers to the process where

minerals dissolve in water, leading to the release of some ions into the water while others remain as solid residues (Belkhir et al. 2010). This can affect the overall chemical composition of the groundwater. In general, the distribution of diverse clay minerals (kaolinite and gibbsite), unrestricted groundwater flow caused by unconsolidated rocks, incongruent mineral dissolution, and the combined impacts of the mineral stability diagram all work together to define the groundwater chemistry in the Tano River Basin. The total hydrogeochemical properties of the groundwater are influenced by interactions between these components. Understanding the above is essential for managing water resources, identifying possible problems with groundwater quality, and selecting appropriate land-use and water management strategies.

4.4 Groundwater and human health risk

This section compares carcinogenic and non-carcinogenic health hazards associated with drinking groundwater (Table 15). The hazard quotient (HQ), which is determined by contrasting contaminant intake through skin contact and ingestion (Li and Zhang 2010; Wu et al. 2009; De Miguel et al. 2007; USEPA 2004), is used to quantify potential non-carcinogenic risks. Concerns over non-carcinogenic health effects may surface if HQ exceeds 1. In order to calculate potential non-carcinogenic risks from all relevant pathways, the health Index (HI) is used. The study found that 18 trace elements pose little hazard in borehole water for both adults and children, with HQ_{ing} and HQ_{derm} values below 1 (Table 15). The highest contributor to chronic risk is Cr for both children and adults, with a HQ_{derm} value of 0.46. Chromium, an element linked to gold deposits (Fu et al. 2017), is a significant contributor to chronic risk in the Tarkwa mining area (Seidu and Ewusi 2020). The high toxicity of Cr makes it crucial to use it for groundwater contamination control and public health in the study area. Drinking Cr-contaminated borehole water can cause severe skin rashes, lung cancer, and other serious illnesses (WHO 2011).

5 Conclusion

In conclusion, this study has identified significant spatial variations in borehole depths, with deeper boreholes primarily concentrated in the northeastern and southeastern zones. The borehole yields have revealed a strong relationship with geological formations, particularly in areas overlying the Apollonian Formation, characterized by highly porous and permeable rocks. The obtained transmissivity values have highlighted high transmissivity zones in the southern, southeastern, eastern, and southwestern

regions, and low transmissivity zones in the northeastern, central, and southern areas, signalling lower groundwater availability. The hydraulic conductivity values have demonstrated the suitability of various areas across the basin for groundwater recharge, with high hydraulic conductivity zones in the southern, southeastern, eastern, and southwestern areas. The highest specific capacity values were seen in the southern zone of the study area. The groundwater flow direction revealed a consistent pattern of flow from higher hydraulic head recharge areas in the north-west, southern, and western regions toward lower hydraulic head discharge areas in the south-east and western regions. The study has also demonstrated that the groundwater in the Tano River Basin generally falls within the category of freshwater based on its low total dissolved solutes (TDS) and electrical conductivity (EC) values, indicating minimal contamination and favourable hydraulic parameters (hydraulic conductivity, etc.) in the aquifers. Microbiological analysis identified areas of concern, with elevated levels of *E. coli* and coliforms in certain boreholes, particularly those developed in the aquifer of the Apollonian Formation. Additionally, trace element analysis detected elevated concentrations of elements such as iron, chromium, aluminium, nickel, arsenic, and lead in some boreholes, exceeding WHO (2011) standards. Overall, the study's water quality index (WQI) assessment revealed spatial variations in groundwater quality, ranging from excellent to extremely poor, with areas underlain by the Apollonian Formation exhibiting lower groundwater quality. The PCA results revealed geogenic processes, associated with the underlying geology, significantly influencing the chemistry of the groundwater. In addition, anthropogenic sources and mineral dissolution played a vital role in the chemistry of the groundwater. According to the health risk assessment, 18 trace elements (As, Ba, B, Cd, Cr, Co, Cu, Pb, Mn, Ni, Se, Ag, Sr, Ti, V, Zn, Al, and Fe) in the borehole water samples are of low concern for both adults and children, as their HQ values were below the threshold of 1, signifying a minimal risk of non-carcinogenic health effects from these contaminants. Notably, chromium (Cr) emerged as the most significant contributor to chronic health risk for both age groups, with an HQ_{derm} value of 0.46.

6 Recommendation

- Moving forward, continued research and monitoring are necessary to deepen the understanding of groundwater contaminants and their potential health impacts in the Tano River Basin.
- Additionally, the development and application of innovative technologies for groundwater remediation

and risk mitigation should be pursued by policymakers in Ghana to safeguard human health and preserve the quality of this vital natural resource.

- Collaboration with local stakeholders and the adoption of a multidisciplinary approach is required in order to ensure the success of future groundwater studies and pave the way for informed decision-making in the pursuit of achieving SDG 6 in the Tano River Basin in Ghana.

Acknowledgements The authors are grateful to ICTP/IAEA Step Educational Programme, staff and lecturers of Ca Foscari University of Venice, Italy, Ghana Atomic Energy Commission and Ghana Educational Trust Fund (GETFUND), the district assembly officer, Hon Kwasi Bonzoh for their support and assistance.

Author contributions AK-ME: Conceptualization, methodology, sampling, analysis, and writing read and approved the manuscript. BB-Y: Supervision of the entire research work and manuscript, read and approved the manuscript. AE: Supervision of the entire research work and manuscript, read and approved the manuscript. ES-Y: Data analysis and interpretation, read and approved the manuscript. DS: Data analysis and interpretation, read and approved the manuscript. CT: Supervision of Laboratory analysis and interpretation, read and approved the manuscript. GC: Supervision of Laboratory analysis and interpretation, read and approved the manuscript. DA-P: Review and Proof read the manuscript and worked on the geology, read and approved the manuscript. LPC: Proof read the manuscript, read and approve the manuscript.

Funding The authors declare that no funds were received during the manuscript preparation.

Data availability All data analysed during this research work are summarized and included in this published work but contact the corresponding author for all detailed data.

Declarations

Conflict of interest The authors of this manuscript declare no competing interests.

Ethics approval and consent to participate Not applicable.

Consent for publication Not applicable.

References

- Adamu C, Nganje T, Edet A (2015) Heavy metal contamination and health risk assessment associated with abandoned barite mines in Cross River State, southeastern Nigeria. *Environ Nanotechnol Monit Manag* 3:10–21
- Affum AO, Osae SD, Kwaansa-Ansah EE, Miyittah MK (2020) Quality assessment and potential health risk of heavy metals in leafy and non-leafy vegetables irrigated with groundwater and municipal-waste-dominated stream in the Western Region, Ghana. *Heliyon* 6(12):e05829. <https://doi.org/10.1016/j.heliyon.2020.e05829>
- Anim-Gyampo GK, Anornu EK, Appiah-Adjei SKA (2019) Quality and health risk assessment of shallow groundwater aquifers within the Atankwidi basin of Ghana. *Groundw Sustain Dev* 9:100217. <https://doi.org/10.1016/j.gsd.2019.100217>
- APHA (1998) Standard methods for the examination of water and wastewater, 20th edn. American Public Health Association, American Water Works Association and Water Environmental Federation, Washington
- Appelo C, Postma D (2005) *Geochemistry, groundwater and pollution*, 2nd edn. Balkema, Rotterdam. <https://doi.org/10.1201/9781439833544>
- Armah F (2014) Relationship between coliform bacteria and water chemistry in groundwater within gold mining environments in Ghana. *Water Qual Expo Health* 5:183–195. <https://doi.org/10.1007/s12403-014-0110-1>
- Atta-Peters D, Garrey P (2014) Source rock evaluation and hydrocarbon potential in the Tano Basin, South Western Ghana, West Africa. *Int J Oil Gas Coal Eng* 2(5):66–77. <https://doi.org/10.11648/j.ogce.20140205.11>
- Belkhir L, Boudoukha A, Mouni L, Baouz T (2010) Multivariate statistical characterization of groundwater quality in Ain Azel Plain, Algeria. *Afr J Environ Sci Technol* 4:526–534. <https://doi.org/10.4314/ajest.v4i8.71307>
- Belkhir L, Abderrahmane B, Mouni L, Baouz T (2012) Multivariate Statistical Characterization of Groundwater Quality in Ain Azel Plain, Algeria. *Afr J Environ Sci Technol* 4:526–534. <https://doi.org/10.4314/ajest.v4i8.71307>
- Boateng TK, Opoku F, Akoto O (2018) Quality of leachate from the Oti Landfill Site and its effects on groundwater: a case history. *Environ Earth Sci*. <https://doi.org/10.1007/s12665-018-7626-9>
- Bowell RJ, McEldowney A, Mathew WA, Bwankuzo M (1996) Biogeochemical factors affecting groundwater quality in central Tanzania. *Geol Soc Lond Spec Publ* 113(1):107–130
- Cobbina SJ, Duwiejuah AB, Quansah R, Obiri S, Bakobie N (2015) Comparative assessment of heavy metals in drinking water sources in two small-scale mining communities in northern Ghana. *Int J Environ Res Public Health*. <https://doi.org/10.3390/ijerph120910620>
- De Miguel A, Iribarren I, Chacon E, Ordonez A, Charlesworth S (2007) Risk-based evaluation of the exposure of children to trace elements in playgrounds in Madrid (Spain). *Chemosphere* 66(3):505–513. <https://doi.org/10.1016/j.chemosphere.2006.05.065>
- Doyi I, Essumang D, Gbeddy G, Dampare S, Kumassah E, Saka D (2018) Spatial distribution, accumulation and human health risk assessment of heavy metals in soil and groundwater of the Tano Basin, Ghana. *Ecotoxicol Environ Saf*. <https://doi.org/10.1016/j.ecoenv.2018.09.015>
- Drever JI (1988) *The geochemistry of natural waters*, 2nd edn. Prentice-Hall, Englewood Cliffs, p 437
- Dzigbodi-Adjimah K, Asamoah ND (2009) The geology of the gold deposits of Prestea Gold Belt of Ghana. *Ghana Min J* 11:7–18
- Edjah AKM, Akiti TT, Osae S et al (2015) Hydrogeochemistry and isotope hydrology of surface water and groundwater systems in the Ellembelle district, Ghana, West Africa. *Appl Water Sci* 7:609–623. <https://doi.org/10.1007/s13201-015-0273-3>
- Edjah AKM, Banoeng-Yakubo B, Akiti TT et al (2019) Characterization of water chemistry in some communities of the Lower Tano river basin, Ghana, West Africa. *Arab J Geosci* 12:160. <https://doi.org/10.1007/s12517-019-4305-4>
- Edjah AK, Banoeng-Yakubo B, Akiti TT, Doku-Amponsah K, Duah AA, Sakyi-Yeboah E, Kippo JV, Amadu I, Ibrahim K (2021) The use of statistical methods to assess groundwater contamination in the Lower Tano river basin, Ghana, West Africa. *Environ Monit Assess*. <https://doi.org/10.1007/s10661-021-09514-z>
- Edmunds W, Smedley PL (1996) Groundwater geochemistry and health: an overview. *Geol Soc Lond Spec Publ* 113:91–105. <https://doi.org/10.1144/GSL.SP.1996.113.01.08>

- Egbi CD, Anornu GK, Ganyaglo SY, Appiah-Adjei EK, Li SL, Dampare SB (2020) Nitrate contamination of groundwater in the Lower Volta River Basin of Ghana: sources and related human health risks. *Ecotoxicol Environ Saf* 191:110227. <https://doi.org/10.1016/j.ecoenv.2020.110227>
- Elango L, Kannan R (2007) Rock–water interaction and its control on chemical composition of groundwater. In: Sarkar D, Datta R, Hannigan R (eds) *Concepts and applications in environmental geochemistry*. Elsevier Science, Amsterdam, pp 229–246
- Engström E, Balfors B, Mörtberg U, Thunvik R, Gaily T, Mangoldc M (2015) Prevalence of microbiological contaminants in groundwater sources and risk factor assessment in Juba, South Sudan. *Sci Total Environ* 515–516:181–187
- Freeze RA, Cherry JA (1979) *Groundwater*, vol 7632. Prentice-Hall Inc., Englewood Cliffs, p 604
- Fu J, Liu S, Wang M, Chen X, Guo B, Hu F (2017) Late neoproterozoic monzogranitic-syenogranitic gneisses in the Eastern Hebei–Western Liaoning Province, North China Craton: petrogenesis and implications for tectonic setting. *Precamb Res* 303:392–413. <https://doi.org/10.1016/j.precamres.2017.05.0>
- Gastmans D, Chang H, Hutcheon I (2010) Groundwater geochemical evolution in the northern portion of the Guarani Aquifer System (Brazil) and its relationship to diagenetic features. *Appl Geochem* 25:16–33. <https://doi.org/10.1016/j.apgeochem.2009.09.024>
- Ghana Statistical Service (GSS) (2013) 2010 Population and Housing Census: Regional Analytical Report Western Region. GSS, Accra
- Gyamfi E, Appiah-Adjei EK, Adjei KA (2019) Potential heavy metal pollution of soil and water resources from artisanal mining in Kokoteasua, Ghana. *Groundw Sustain Dev* 8:450–456. <https://doi.org/10.1016/j.gsd.2019.01.007>
- Health Canada (2018) Strontium in drinking water-Guideline Technical Document for public consultation. <https://www.canada.ca/en/health-canada/programs/consultation-strontium-drinking-water/document.html>
- Hirdes W, Davis DW, Eisenlohr BN (1992) Reassessment of Proterozoic granitoid ages in Ghana on the basis of U/Pb zircon and monazite dating. *Precamb Res* 56:89–96
- (2022). <https://allafrica.com/stories/202207060262.html>
- Isa NM, Aris AZ, Sulaiman WN (2012) Extent and severity of groundwater contamination based on hydrochemistry mechanism of sandy tropical coastal aquifer. *Sci Total Environ* 438:414–425. <https://doi.org/10.1016/j.scitotenv.2012.08.069>
- Johnson CR, Greenkorn RA, Woods EG (1966) Pulse-testing: a new method for describing reservoir flow properties between wells. *J Pet Technol* 18(12):1–599
- Kaiser HF (1960) The application of electronic computers to factor analysis. *Educ Psychol Meas* 20(1):141–151
- Kesse GO (1985) *The mineral and rock resources of Ghana*. Balkema, Rotterdam
- Khashgij MS, El Maghraby MMS (2013) Evaluation of groundwater resources for drinking and agricultural purposes, Abar Al Mashi area, south Al Madinah Al Munawarah City, Saudi Arabia. *Arab J Geosci* 6(10):3929–3942. <https://doi.org/10.1007/s12517-012-0649-8>
- Kolsi SH, Bouri S, Hachicha W, Dhia HB (2013) Implementation and evaluation of multivariate analysis for groundwater hydrochemistry assessment in arid environments: a case study of Hajeb Elyoun Jelma, Central Tunisia. *Environ Earth Sci* 70:2215–2224
- Leube A, Hirdes W, Mauer R, Kesse GO (1990) The early Proterozoic Birimian Super group of Ghana and some aspects of its associated gold mineralization. *Precamb Res* 46(1–2):139–165. [https://doi.org/10.1016/0301-9268\(90\)90070-7](https://doi.org/10.1016/0301-9268(90)90070-7)
- Li S, Zhang Q (2010) Risk assessment and seasonal variations of dissolved trace elements and heavy metals in the Upper Han River, China. *J Hazard Mater* 181(1–3):1051–1058. <https://doi.org/10.1016/j.jhazmat.2010.05.120>
- Lutterodt G, Van de Vossenberg J, Hoiting Y, Kamara AK, Oduro-Kwarteng S, Foppen JWA (2018) Microbial groundwater quality status of hand-dug wells and boreholes in the Dodowa Area of Ghana. *Int J Environ Res Public Health* 15:730. <https://doi.org/10.3390/ijerph15040730>
- Magesh NS, Krishnakumar S, Chandrasekar N, Soundranayagam JP (2013) Groundwater quality assessment using WQI and GIS techniques, Dindigul district, Tamil Nadu. *India Arab J Geosci* 6(11):4179–4189
- Martyn CN, Barker DJP, Osmond C, Harris EC, Edwardson JA, Lacey RF (1989) Geographical relation between Alzheimer's disease and aluminium in drinking water. *Lancet* 1:59–62
- Nganje TN, Agbor EE, Adamu CI, Ukpong AJ et al (2019) Public health challenges as a result of contaminated water sources in Kumba, Cameroon. *Environ Geochem Health* 42(4):1167–1195. <https://doi.org/10.1007/s10653-019-00375-7>
- Nkansah MA, Ofosuah J, Boaky S (2010) Quality of groundwater in the Kwahu West District of Ghana. *Am J Sci Ind Res* 1:578–584. <https://doi.org/10.3923/erj.2011.31.37>
- Obasi PN, Akudinobi BB (2020) Potential health risk and levels of heavy metals in water resources of lead–zinc mining communities of Abakaliki, southeast Nigeria. *Appl Water Sci* 10:184. <https://doi.org/10.1007/s13201-020-01233-z>
- Omeka ME, Egbueri JC (2022) Hydrogeochemical assessment and health-related risks due to toxic element ingestion and dermal contact within the Nnewi–Awka urban areas, Nigeria. *Environ Geochem Health*. <https://doi.org/10.1007/s10653-022-01332-7>
- Piper AM (1944) A graphic procedure in the geochemical interpretation of water-analyses. *Trans Am Geophys Union* 25(6):914–928. <https://doi.org/10.1029/TR025i006p00914>
- Preda M, Cox M (2000) Sediment–water interaction, acidity and other water quality parameters in a subtropical setting, Pimpama River, southeast Queensland. *Environ Geol* 39(3/4):319–329. <https://doi.org/10.1007/s002540050011>
- Qin R, Wu Y, Xu Z, Xie D, Zhang C (2013) Assessing the impact of natural and anthropogenic activities on groundwater quality in coastal alluvial aquifers of the lower Liaohe River Plain, NE China. *Appl Geochem* 31:142–158
- Radford M, Yunesian R, Nabizadeh H, Biglari S, Nazmara M, Hadi N, Yousefi M, Yousefi A, Abbasnia AH (2019) Mahvi Drinking water quality and arsenic health risk assessment in Sistan and Baluchestan, Southeastern Province, Iran. *Hum. Ecol. Assess* 25(4):949–965. <https://doi.org/10.1080/10807039.2018.1458210>
- Rahman MM, Islam MA, Bodrud-Doza M, Muhib MI, Zahid A, Shammi M, Tareq SM, Kurasaki M (2017) Spatio-temporal assessment of groundwater quality and human health risk: a case study in Gopalganj. *Expo Health*. <https://doi.org/10.1007/s12403-017-0253-y>
- Ranjan RK, Ramanathan AL, Parthasarathy P, Kumar A (2013) Hydrochemical characteristics of groundwater in the plains of Phalgu River in Gaya, Bihar. *India Arab J Geosci* 6(9):3257–3267
- Saxena V, Mondal NC, Singh V (2004) Identification of sea-water ingress using strontium and boron in Krishna Delta, India. *Curr Sci* 86:586–590
- Seidu J, Ewusi A (2020) Assessment of groundwater quality and health risk of heavy metals: a study from the Tarkwa Mining Area. *Ghana Min J* 20:1–10. <https://doi.org/10.4314/gm.v20i2.1>
- Sjöström J (1993) Ionic composition and mineral equilibria of acidic groundwater on the west coast of Sweden. *Geo* 21:219–226. <https://doi.org/10.1007/BF00775911>
- Smedley PL, Kinniburgh DG (2002) A review of the source, behavior and distribution of arsenic in natural waters. *Appl Geochem* 17:517–568. [https://doi.org/10.1016/S0883-2927\(02\)00018-5](https://doi.org/10.1016/S0883-2927(02)00018-5)

- Subba Rao N (2002) Geochemistry of groundwater in parts of Guntur district Andhra Pradesh, India. *Environ Geol* 41:552–562
- Tano Basin IWRM Plan, WRC (Water resources commission) (2012). <https://www.wrc-gh.org/>
- Taylor PN, Moorbath S, Leube A, Hirdes W (1992) Early Proterozoic crustal evolution in the Birimian of Ghana: constraints from geochronology and isotope geology. *Precambr Res* 56:97–111
- Theis CV (1934) Progress report on the ground water supply of Lea County, New Mexico: New Mexico state Engineer, 11th Biennial Report, 1932–1934, pp 121–134
- USEPA (United States Environmental Protection Agency) (2004). Risk assessment guidance for superfund volume I: Human Health Evaluation Manual (Part E, Supplemental Guidance for Dermal Risk Assessment), Final. Office of Superfund Remediation and Technology Innovation, U.S. Environmental Protection Agency
- USEPA (1986) Ambient Water Quality Criteria for Bacteria-1986. EPA-440/5-84-002. Washington, DC: US Environmental Protection Agency: Office of Water Regulations and Standards, Criteria and Standards Division
- Water Research Commission (WRC) Ghana (2010) Tano River basin – Integrated Water Resources Management Plan. Retrieved from <http://doc.wrc-gh.org>
- Weaver MCJ, Cave L, Talma AS (2007) Groundwater sampling: a comprehensive guide for sampling method, WRC Report No TT 303/07, pp 168.
- World Health Organization (WHO) (2017) World Health Statistics 2017: Monitoring Health for the SDGs, Sustainable Development Goals. WHO, Geneva
- WHO (2011, 2017) Guidelines for drinking-water quality. 4th, 5th edn. Environmental Health Criteria, Geneva. <http://www.who.int>
- Wu CM, Yeh JTC, Zhu J, Lee TH, Hsu NS, Chen CH, Sancho AF (2005) Traditional analysis of aquifer tests: comparing apples to oranges? *Water Resour Res* 41:W09402. <https://doi.org/10.1029/2004WR003717>
- Wu B, Zhao DY, Jia HY, Zhang Y, Zhang XX, Cheng SP (2009) Preliminary risk assessment of trace metal pollution in surface water from Yangtze River in Nanjing Section, China. *Bull Environ Contam Toxicol* 82(4):405–409. <https://doi.org/10.1007/s00128-008-9497-3>
- Zumlot T, Batayneh A, Nazal Y, Ghrefat H, Mogren S, Zaman H, Qaisy S (2013) Using multivariate statistical analyses to evaluate groundwater contamination in the northwestern part of Saudi Arabia. *Environ Earth Sci* 70(7):3277

Springer Nature or its licensor (e.g. a society or other partner) holds exclusive rights to this article under a publishing agreement with the author(s) or other rightsholder(s); author self-archiving of the accepted manuscript version of this article is solely governed by the terms of such publishing agreement and applicable law.